Report of the AAPM Task Group No. 105: Issues associated with clinical implementation of Monte Carlo-based photon and electron external beam treatment planning

Indrin J. Chetty[a)]
University of Michigan, Ann Arbor, Michigan 48109
and University of Nebraska Medical Center, Omaha, Nebraska 68198-7521

Bruce Curran
University of Michigan, Ann Arbor, Michigan 48109

Joanna E. Cygler
Ottawa Hospital Regional Cancer Center, Ottawa, Ontario K1H 1C4, Canada

John J. DeMarco
University of California, Los Angeles, Callifornia 90095

Gary Ezzell
Mayo Clinic Scottsdale, Scottsdale, Arizona 85259

Bruce A. Faddegon
University of California, San Francisco, California 94143

Iwan Kawrakow
National Research Council of Canada, Ottawa, Ontario K1A 0R6, Canada

Paul J. Keall
Stanford University Cancer Center, Stanford, California 94305-5847

Helen Liu
University of Texas MD Anderson Cancer Center, Houston, Texas 77030

C.-M. Charlie Ma
Fox Chase Cancer Center, Philadelphia, Pennsylvania 19111

D. W. O. Rogers
Carleton University, Ottawa, Ontario K1S 5B6, Canada

Jan Seuntjens
McGill University, Montreal, Quebec H3G 1A4, Canada

Daryoush Sheikh-Bagheri
The Regional Cancer Center, Erie, Pennsylvania 16505

Jeffrey V. Siebers
Virginia Commonwealth University, Richmond, Virginia 23298

(Received 11 April 2006; revised 11 July 2007; accepted for publication 18 September 2007; published 27 November 2007)

The Monte Carlo (MC) method has been shown through many research studies to calculate accurate dose distributions for clinical radiotherapy, particularly in heterogeneous patient tissues where the effects of electron transport cannot be accurately handled with conventional, deterministic dose algorithms. Despite its proven accuracy and the potential for improved dose distributions to influence treatment outcomes, the long calculation times previously associated with MC simulation rendered this method impractical for routine clinical treatment planning. However, the development of faster codes optimized for radiotherapy calculations and improvements in computer processor technology have substantially reduced calculation times to, in some instances, within minutes on a single processor. These advances have motivated several major treatment planning system vendors to embark upon the path of MC techniques. Several commercial vendors have already released or are currently in the process of releasing MC algorithms for photon and/or electron beam treatment planning. Consequently, the accessibility and use of MC treatment planning algorithms may well become widespread in the radiotherapy community. With MC simulation, dose is computed stochastically using first principles; this method is therefore quite different from conventional dose algorithms. Issues such as statistical uncertainties, the use of variance reduction techniques, the

ability to account for geometric details in the accelerator treatment head simulation, and other features, are all unique components of a MC treatment planning algorithm. Successful implementation by the clinical physicist of such a system will require an understanding of the basic principles of MC techniques. The purpose of this report, while providing education and review on the use of MC simulation in radiotherapy planning, is to set out, for both users and developers, the salient issues associated with clinical implementation and experimental verification of MC dose algorithms. As the MC method is an emerging technology, this report is not meant to be prescriptive. Rather, it is intended as a preliminary report to review the tenets of the MC method and to provide the framework upon which to build a comprehensive program for commissioning and routine quality assurance of MC-based treatment planning systems. © *2007 American Association of Physicists in Medicine*. [DOI: 10.1118/1.2795842]

Key words: Monte Carlo dose calculation, clinical treatment planning, experimental verification

TABLE OF CONTENTS

I. INTRODUCTION

I.A. Motivation

The accuracy of dose calculations is crucial to the quality of treatment planning and consequently to the doses delivered to patients undergoing radiation therapy.[1] Among other fac-

tors, dose calculations form an integral component in optimizing the therapeutic gain, i.e., maximizing the dose to the tumor for a given normal-tissue dose, for patients treated with radiation. Although the clinical benefit of more accurate dose distributions (i.e., how the improved dose distributions will affect tumor recurrence, i.e., local control, and normal tissue complications) has not been adequately quantified and requires further investigation, evidence exists that dose differences on the order of 7% are clinically detectable.[2] Moreover, several studies have shown that 5% changes in dose can result in 10%–20% changes in tumor control probability (TCP) or up to 20–30% changes in normal tissue complication probabilities (NCTP) if the prescribed dose falls along the steepest region of the dose-effect curves.[3–5] Readers interested in further understanding the need for heterogeneity corrections, among other topics related to dose calculations, are encouraged to read the AAPM Report No. 85,[1] where a comprehensive review of tissue heterogeneity corrections for megavoltage photon beams is provided.

In this report we focus our attention on the Monte Carlo (MC) method, a dose calculation algorithm known to be very accurate when used properly for treatment planning in heterogeneous patient tissues. The issue of lengthy calculation times has traditionally led to the MC method being viewed in the medical physics community as a clinically unfeasible approach. However, the development of MC codes optimized for radiotherapy calculations as well as the availability of much faster and affordable computers, have substantially reduced processing times. These significant advances have led to the clinical use of MC algorithms at some treatment centers and the promised availability of MC photon/electron planning modules among several commercial treatment planning vendors.

In light of the above considerations, MC treatment planning is quickly becoming a reality. An introductory report for the medical physics community on the understanding, implementation, testing, and use of MC algorithms is therefore warranted.

I.B. Objectives for the report

We intend this document to be a preliminary report with the following objectives: (a) to provide an educational review of the physics of the MC method and how it is applied in external beam radiotherapy dose calculations, (b) to describe the role of the MC method in external beam radiotherapy treatment planning process: from the interaction of electrons in the target of the linear accelerator to the deposition of dose in the patient tissues, (c) to describe the issues associated with MC dose calculation within the patient-specific geometry, (d) to discuss the issues associated with experimental verification of MC algorithms, and (e) to discuss the clinical implications of MC calculated dose distributions.

We expect that areas of concern outlined in this report will be further investigated and that more detailed reports providing recommendations on the major issues will be forthcoming.

I.C. Organization of the report

Following the introductory section (Sec. I) we begin in Sec. II with a review of the MC method as it applies to photon and electron transport. We include in this section an overview of MC simulation from the accelerator treatment head to the patient as well as a discussion of variance reduction techniques and efficiency-enhancing methods integral to MC calculations in radiotherapy. Section III begins with a review of the major MC codes being used in clinical application and is followed by detailed discussions on accelerator treatment head modeling and patient-specific treatment planning. This section concludes with the topic of experimental verification, in which guidance is provided on the types of tests needed to verify the accuracy of MC dose calculation algorithms. In Sec. IV we provide a review of recent studies demonstrating the potential clinical impact of MC dose calculations in comparison with conventional algorithms. Finally, we conclude in Sec. V with a summary of the recommendations from this task group report.

II. THE MONTE CARLO METHOD IN RADIOTHERAPY DOSE CALCULATIONS

II.A. Definition of the MC method and historical background

Most generally, the MC technique is a statistical method for performing numerical integrations. MC simulations are employed in many areas of science and technology. Although a method based on random sampling was discussed as early as 1777 by Buffon,[6] the MC technique as we know it today was first developed and named at the end of the second world war. The motivation was to apply MC techniques to radiation transport, specifically for nuclear weapons.[7] The driving forces for the initial idea appear to have been Stanislaw Ulam and John von Neumann who saw the development of ENIAC, the first electronic computer, as an ideal opportunity to develop new applications of statistical sampling. The developments of MC techniques and computers have been closely intertwined ever since, with an exponential increase of the application of MC simulations since digital computers became widely available in the 1950s and 1960s.

Modeling of particle transport problems is ideally suited for the use of MC methods and has been described by Rogers and Bielajew as follows: "The Monte Carlo technique for the simulation of the transport of electrons and photons though bulk media consists of using knowledge of the probability distributions governing the individual interactions of electrons and photons in materials to simulate the random trajectories of individual particles. One keeps track of physical quantities of interest for a large number of histories to provide the required information about the average quantities."[8] As a technique for calculating dose in a patient the underlying physical basis is much simpler in concept than analytic algorithms because the MC method consists of a straightforward simulation of reality and does not involve complex approximations nor models of dose deposition, but only a knowledge of the physics of the various interactions which

have been well understood for over 50 years in most cases. While some of these interactions may be complex to simulate in detail, the basic ideas of each interaction, e.g., an electron giving off a bremsstrahlung photon, are well understood by medical physicists and, hence, the overall process is easy to comprehend.

Although MC was used in several particle physics applications to simulate electron-photon showers in the 1950s, the seminal paper in the field was that of Berger in 1963,[9] in which he described the condensed history technique for electron transport. This technique is the basis of all modern electron-photon transport MC codes relevant to medical physics. The ETRAN code, based on these ideas[10] was developed by Berger and Seltzer and now forms the basis of electron transport in the MCNP code.[11] The release of the EGS4 MC code system in 1985[12] served as a catalyst for the application of the MC method in radiotherapy calculations of dose and dosimeter response. The work of Petti *et al.*,[13] Mohan *et al.*,[14] and Udale[15] being early examples of the use of the EGS MC code system[12,16,17] to simulate medical linear accelerators. Even without the direct use of MC simulations, the MC method already plays a significant role in radiotherapy treatment planning since the energy deposition kernels used in convolution/superposition algorithms have been calculated using MC techniques. Linear accelerator calibration protocols (e.g., AAPM's TG-51)[18] use factors derived from MC simulations. MC-based calculations are also used in the design of treatment head components.[19,20]

Although it has only recently become practical, for over two decades the application of MC techniques to radiation treatment planning has been quite clear.[21,22] The widely used BEAM code system[23] is a pair of EGS4 (now EGSnrc)[17] user codes for simulating radiation transport in accelerators and in patients represented by CT data sets. These relatively easy to use tools have sparked intense research in MC-based radiotherapy treatment planning and have lead to two comprehensive reviews of accelerator simulations by Ma and Jiang[24] and Verhaegen and Seuntjens.[25] Kawrakow and Fippel, among others, have provided the breakthroughs which have made clinical treatment planning feasible, as discussed in Sec. III A. The fast MC codes being developed commercially are almost all based on the results of this collaboration. As this report is being written, the first commercial MC systems have already been introduced into routine clinical treatment planning for electrons[26] and photons.[27]

II.B. Monte Carlo simulation of electron and photon transport

The following material represents a very brief introduction into the MC simulation of electron and photon transport. For more details the reader is referred to the reviews available in the literature.[8,28–31] Another source for detailed information is the documentation accompanying some of the general purpose codes, for instance, the EGSnrc,[17] MCNP,[32] and GEANT4 (Ref. 33) manuals, and the PENELOPE paper.[34]

In the energy range of interest for external beam radiotherapy (megavoltage range), photons interact with surrounding matter via four main processes: incoherent (Compton) scattering with atomic electrons, pair production in the nuclear or electron electromagnetic field, photoelectric absorption, and coherent (Rayleigh) scattering. The first three collision types transfer energy from the photon radiation field to electrons or positrons. In most cases Compton scattering is the dominant interaction, although pair production becomes increasingly important with increasing energy, and may even dominate at higher energies in high-Z components of the treatment head of medical linear accelerators.

When electrons traverse matter, they undergo a large number of elastic interactions and lose energy by two main processes: inelastic collisions with atoms and molecules and radiative interactions. Inelastic collisions result in excitations and ionizations. Ionizations lead to secondary electrons, sometimes referred to as "δ particles". Radiative energy losses, which occur in the form of bremsstrahlung and positron annihilation, transfer energy back to photons and lead to the coupling of the electron and photon radiation fields. One therefore speaks of coupled electron-photon showers.

The electron-photon macroscopic radiation field can be described mathematically by a coupled set of integrodifferential transport equations. These transport equations are prohibitively complicated thereby excluding an analytical treatment except under severe approximations. The MC technique is a solution method that can be applied for any energy range and underlying geometry and material composition.

A solution of the transport problem of particles in matter, which is exact within the existing knowledge of the elementary collision processes, can be obtained by an analog MC simulation. In an analog simulation all particle interactions with surrounding atoms and molecules are explicitly simulated, including those of secondary particles created in the collisions. An analog MC technique is therefore a faithful simulation of physical reality on a digital computer: particles (photons for example) are "born" according to distributions describing the source, they travel a certain distance, determined by a probability distribution, to the site of a collision, and scatter into another energy and/or direction state, possibly creating additional particles. These photons eventually "die" as a result of pair production or photoelectric events or when they Compton scatter to energies below a predetermined low-energy photon cutoff, often called PCUT. Analog simulations, often referred to as "event-by-event" or "interaction-by-interaction" techniques, are typically used for the transport of neutral particles. The analog simulation of charged particle transport is not practical, due to the large number of interactions they undergo until locally absorbed as the energy of the charged particle falls below the predetermined low-energy limit for tracking charged particles, often call ECUT. All general purpose MC codes therefore employ condensed history schemes for charged particle transport, discussed in more detail in Sec. II B 2.

Within a MC simulation, quantities of interest can be computed by averaging over a given set of particle showers (also referred to as "histories," "cases," "trajectories," or "tracks"). One can calculate both observable (measurable)

quantities, such as dose or a particle spectrum, and quantities that cannot easily be measured such as the fraction of particles originating from a certain component of the treatment head, the dose fraction due to scattered photons, etc. Although there are techniques for scoring quantities at a point when using Monte Carlo techniques, in treatment planning applications, it is usual to score quantities (dose mainly) averaged over some finite volume or voxel. As the voxel size is increased, for a given statistical uncertainty the total calculation time will decrease, but the spatial resolution is reduced (see Sec. III D 6 for more discussion). Another important aspect of MC calculations is the presence of statistical uncertainties due to the statistical nature of the method, which is discussed in more detail in Sec. III D 1.

II.B.1. Analog simulations

An analog simulation of particle transport consists of four main steps:

(1) Select the distance to the next interaction.
(2) Transport the particle to the interaction site taking into account geometry constraints.
(3) Select the interaction type.
(4) Simulate the selected interaction.

Steps 1–4 are repeated until the original particle and all secondary particles leave the geometry or are locally absorbed. A particle is considered to be locally absorbed when its energy falls below a specified threshold energy.

Step 1 is based on the probability, $p(r)dr$, that a particle interacts in an interval dr at a distance r from its initial position

$$p(r)dr = e^{-\mu r}\mu dr, \tag{1}$$

where μ is the linear attenuation coefficient (number of interactions per unit length). A random distance r distributed according to $p(r)$ can be sampled using the so-called inverse-transform method, which equates the cumulative probability of $p(r)$ with a random number ξ distributed uniformly between zero and unity

$$\int_0^r p(r')dr' = \xi \Rightarrow r = -\frac{\ln(1-\xi)}{\mu}. \tag{2}$$

Step 2 involves basic ray tracing, which requires a geometry model that can provide the medium and mass density of a region together with a computation of the distance to the next geometry boundary along the particle trajectory.

Step 3 is similar to step 1 except that now the probability distribution function is discrete, i.e., it involves a fixed number of final states i, corresponding to an interaction of type i. Suppose that the cross section for interaction of type i is denoted by σ_i and the total cross section by $\sigma=\Sigma\sigma_i$. A direct application of the inverse-transform method for n interaction types yields interaction *1* if $\xi \leq \sigma_1/\sigma$, else interaction *2* if $\xi \leq (\sigma_1+\sigma_2)/\sigma$, else interaction n, if $\xi \leq (\sigma_1+\sigma_2+\cdots+\sigma_n)/\sigma$.

Perhaps the most difficult part is step 4, where one must sample energy/direction changes from the differential cross section of the selected process. The manuals of the popular general purpose codes[17,32–34] provide details of the methods employed for the relevant photon interactions.

Based on the above discussion it should be clear that an analog MC simulation is conceptually quite straightforward.

II.B.2. Condensed history simulations

The condensed history technique was first described comprehensively in the pioneering work by Berger.[9] It is based on the observation that the vast majority of electron interactions lead to very small changes in the electron energy and/or direction. Many such "small-effect" interactions can therefore be grouped into relatively few condensed history "steps" and their cumulative effect taken into account by sampling energy, direction, and position changes from appropriate distributions of grouped single interactions, e.g., multiple scattering, stopping power, etc. Berger defined two main classes of condensed history implementations. In a class I scheme all collisions are subject to grouping. The effect of secondary particle creation above specified threshold energies are taken into account after the fact (i.e., independently of the energy actually lost during the step) by setting up and transporting the appropriate number of secondary particles. In this way the correlation between large energy losses and secondary particle creation is lost. In a class II scheme interactions are divided into "hard" (sometimes also referred to as "catastrophic") and "soft" collisions. Soft collisions are subject to grouping as in a class I scheme; hard collisions are explicitly simulated in an analog manner.

A class II scheme can be described with the same four basic steps that make up an analog simulation. The two main differences are that only hard collisions are included and that step 2 is much more difficult because the particles do not move on straight lines and because it involves the selection of energy, direction, and position changes from multiple scattering distributions. It is also frequently necessary to divide the distance between catastrophic interactions into shorter condensed history steps to guarantee the accuracy of the simulation. As in an analog simulation there is a transport threshold energy. Particle transport thresholds are often the same as the particle production thresholds dividing hard and soft collisions, but this is not a necessary condition.

A class II MC simulation is illustrated in Fig. 1. The upper portion shows a complete electron track including secondary electrons and photons (shown with dashed lines and not including their interactions) with energies above the hard collision thresholds. The lower portion is a magnified view of the shaded box. The actual curved path has been simulated using four condensed history steps. The filled circles and arrows show the positions and directions at the beginning of the steps. The shaded area around the electron track indicates the region where the energy of subthreshold secondary particles is in reality deposited. If this volume is small compared to the calculation resolution (i.e., voxel size in the case of radiotherapy calculations), energy deposition can be considered local and modeled using a restricted stopping power along the electron track. Note that the initial and final posi-

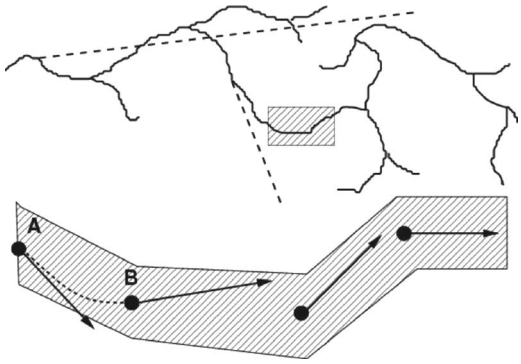

FIG. 1. Illustration of a class II condensed history scheme for electron transport. The upper portion shows a complete electron track including secondary electrons and photons (shown with dashed lines and not including their interactions) with energies above the hard collision thresholds. The lower portion is a magnified view of the shaded box.

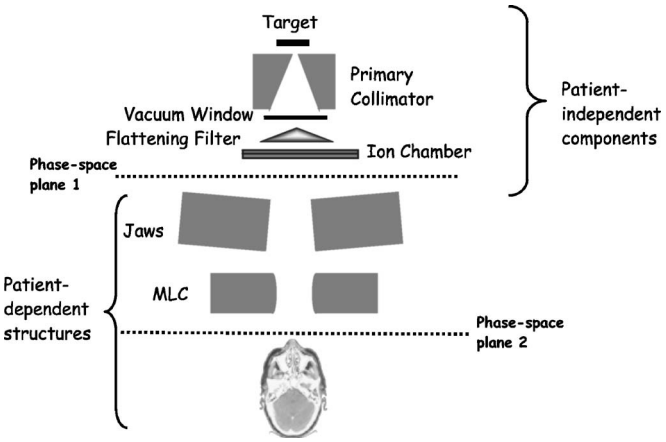

FIG. 2. Illustration of the components of a typical Varian linear accelerator treatment head in photon beam mode. Phase space planes for simulating patient-dependent and patient-independent structures are also represented. For other manufacturers, component structures (such as the jaws, MLC, etc.) may be in different locations, thereby potentially requiring a change in the placement of the phase space scoring planes.

tions of a step are not connected in the figure to highlight the fact that a condensed history implementation does not provide information on how the particle goes from *A* to *B* (the curved dashed line connecting *A* and *B* is a more realistic representation of the trajectory than a straight line from *A* to *B*). This becomes important when the scoring grid is not the same as the underlying geometry grid or when a single condensed history step traverses more than one geometrical region as in some of the fast MC codes specialized for use in radiotherapy.[35–39] This consideration highlights another important aspect of a condensed history simulation, namely the way the transport is performed in the vicinity of or across boundaries between different regions. The EGSnrc code, for instance, utilizes single scattering (i.e., analog) simulation within a certain perpendicular distance from an interface.[40] Although this approach is necessary for accurate simulations of certain types of geometries, it is generally not needed for typical radiotherapy calculations.

Although the condensed history technique makes use of practical MC simulations possible, it introduces the step size as an artificial parameter. Dependencies of the calculated results on the step size have become known as step-size artifacts.[41] Step-size artifacts were a major factor in the early years of most general purpose MC codes. Due to significant theoretical developments in the nineties the condensed history technique is now well understood.[42,43] This has lead to the development of high accuracy condensed history implementations[40,44] and faster MC codes that can compute dose distributions with accuracy comparable to traditional MC packages in a small fraction of the time.[35–39,45]

With charged particle transport one stops tracking the particle's movement at some low-energy cutoff and the choice of the cutoff can affect the calculation in two important ways. The higher the value of the cutoff, the faster the calculation; this can improve the calculation speed significantly. On the other hand, unless great care is taken, stopping at too high a cutoff energy can distort the dose distribution since the "stopped" charged particle might have deposited energy some distance from where its trajectory was terminated. Thus care must be taken in selecting an energy cutoff.

II.C. Overview of Monte Carlo-based radiotherapy dose calculations

It is possible to carry out a single MC simulation in which one starts with the electron exiting from the accelerator structure, follows it and its descendants (e.g., bremsstrahlung photons, knock-on electrons) through the fixed elements of the head (targets or scattering foils, primary collimators, monitor chambers, flattening filters, etc.), the various beam shaping devices which are patient specific (jaws, multileaf collimator (MLC), applicators, cutouts, wedges, compensators), and finally the patient as specified by a CT or some other data set. This tracking of the initial particle and all of its descendants is referred to as a history. As discussed further in Sec. III D 1.1, it is important to include all particles associated with a single initiating electron as part of the same history.

Due to significant improvements in the efficiency of photon beam treatment head simulations,[46] the speed of the complete simulation is such that it is feasible to consider performing the entire calculation for each patient.[47] However, there have been a variety of strategies for dividing such calculations into several steps. The first step, transporting particles through the patient-independent elements, can be inefficient without the use of advanced variance reduction techniques (see Sec. II D). This is especially true for photon beams, since many bremsstrahlung photons generated in the target will strike the primary collimator and not contribute to the beam reaching the patient. One approach to improve the simulation efficiency is to first perform the simulation of the patient-independent structures and to store what is called a phase-space file at a plane just below the fixed elements of the accelerator head (see phase-space plane 1 in Fig. 2). The phase-space file contains phase-space parameters for all particles as they cross the scoring plane. The phase-space parameters consist of the energy, position, direction, charge, and possibly other information such as the region/s of cre-

ation or interaction of particles. The advantage of this approach is that this part of the calculation can be reused as often as necessary. Particles are then transported through the patient specific collimation system and are either stored in another phase-space file at the base of the accelerator (see phase-space plane 2 in Fig. 2) or tracked through the patient in the same simulation. Storing a second phase-space may be more efficient when open fields (e.g., 10×10 cm^2 fields) are used for treatment, however, more commonly, when MLCs are used for beam shaping, the latter approach is likely to be more efficient.

As we will discuss in Sec. III C, the entire phase-space data for the accelerator may also be generated using beam modeling (virtual source model) approaches which do not require direct MC simulation of the accelerator for each treatment. One class of virtual source models is based on characterizing the results of a MC simulation of the accelerator head and another class is based solely on measured beam data such as depth-dose curves, profiles and output ratios. In either case, the patient-dependent components (e.g., the MLC) are simulated using either explicit transport methods or approximate transport methods before detailed transport in the patient.

As with conventional planning methods, experimental verification forms an integral part of the clinical implementation of a MC dose calculation algorithm. MC algorithms will benefit from similar experimental verification procedures as conventional systems, and as such should follow the commissioning procedures detailed in the AAPM TG-53 report[48] and other relevant publications.[49,50] Experimental verification in more complex fields and/or heterogeneous geometries is useful to verify the expected improved accuracy associated with MC calculations in these situations.

II.D. Variance reduction techniques and efficiency enhancing methods

The efficiency, epsilon (ε), of a MC calculation is defined as: $\varepsilon=1/s^2T$, where s^2 is an estimate of the true variance (σ^2) of the quantity of interest and T is the CPU time required to obtain this variance. Since both Ns^2 and T/N are approximately constant, the efficiency is roughly independent of N, the number of histories simulated. There are two ways to improve the efficiency of a given calculation: either decrease s^2 for a given T or decrease T for a given N while not changing the variance. Techniques which improve the efficiency by changing the variance for a given N while not biasing the result (i.e., not changing the expectation value which is the value expected in an infinitely long run) are called variance reduction techniques. Variance reduction techniques often increase the time to simulate a single history and are only useful if the overall efficiency is improved. A given technique may increase the efficiency for some quantities being scored and decrease it for others. In contrast to variance reduction techniques, there are a variety of ways to speed up a given calculation by making an approximation which may or may not affect the final result in a significant way.

Bremsstrahlung splitting and Russian roulette of secondary particles are widely used variance reduction techniques which are especially useful in simulating an accelerator treatment head.[23,46] In the various forms of bremsstrahlung splitting, each time an electron is about to produce a bremsstrahlung secondary, a large number of secondary photons with lower weights are set in motion, the number possibly depending on a variety of factors related to the likelihood of them being in the field. If the number of photons created is selected to minimize those that are not directed toward the patient plane, then there is a further saving in time. Russian roulette can be played whenever there is little interest in a particle resulting from a specific class of events. The low interest particles are eliminated with a given probability, but to ensure an unbiased result, the weights of the surviving particles are increased by the inverse of that probability. A common example is to play Russian roulette with secondary electrons created from photon interactions in treatment head structures. Another variance reduction method, photon forcing, may sometimes be used to enhance the production of electrons in the air downstream of the accelerator. In a photon forcing scheme, the parent photon is forced to interact in a given geometric region and the weights of the resulting particles are adjusted accordingly to maintain an unbiased result.

Range rejection and increasing the energy at which electron histories are terminated (energy cutoffs) are examples of methods which, when used correctly, improve efficiency by decreasing the time per history without significantly changing the results. In range rejection, an electron's history is terminated whenever its residual range is so short that it cannot escape from the current region or reach the region of interest. In most implementations this ignores the possible creation of bremsstrahlung photons while the electron loses energy which means this is an approximate technique. When applied to electrons below a certain energy threshold, this form of range rejection produces the same results in a reduced computing time.[23] It is also possible to implement range rejection in a manner which properly accounts for bremsstrahlung production and thus make it an unbiased variance reduction technique. By stopping tracking of electrons at a higher energy, efficiency can be improved, but this may have an effect on the dose distribution if too high a threshold is used. Playing Russian roulette with particles at energies below a relatively high transport cutoff or with range-rejected particles is a comparable variance reduction technique for reducing the simulation time. However, its implementation is typically more difficult and this has favored the use of range rejection and high transport cutoffs in situations where it is easy to demonstrate that the resulting error is sufficiently small.

There are other variance reduction and efficiency enhancing techniques which collectively have allowed substantial increases in the speed of a calculation. These methods include the reuse of particle tracks,[37] and other adaptations of particle track reuse, such as the simultaneous transport of particle sets (STOPS) approach of Kawrakow,[36] which is a variance reduction technique. For a more comprehensive re-

view of variance reduction and efficiency enhancing techniques, readers are referred to a chapter by Rogers and Bielajew[51] and the papers by Rogers *et al.*[23] and Kawrakow *et al.*[46,52] Other useful references on the influence of variance reduction methods in the context of phantom and patient treatment planning are provided in the articles by Ma *et al.*[53] and Kawrakow and Fippel.[45]

In summary, variance reduction techniques are an important requirement for the use of MC calculations in the clinical setting; without them, calculation times would still be too long for use in most situations. However, inappropriate use of a variance reduction technique can reduce calculation efficiency, thus increasing calculation time. In principle variance reduction techniques, implemented correctly, do not alter the physics and thereby produce unbiased results. Other efficiency improving techniques can significantly alter the accuracy of the calculation if applied inappropriately. Improper implementations can lead to unpredictable results in either case.

It is incumbent upon the medical physicist to understand, at a minimum, those techniques that the user can adjust in a clinical MC algorithm. In addition, tests must be done to show correct implementation of those techniques over the range of clinical situations. Vendors should provide adequate documentation for users to understand the techniques employed and how the implementation was validated.

III. MONTE CARLO SIMULATION OF RADIATION TRANSPORT IN ACCELERATORS AND PATIENTS

III.A. Review of current Monte Carlo codes

A large number of general purpose MC algorithms have been developed for simulating the transport of electrons and photons. Perhaps the most widely used of these in medical physics is the EGS code system.[12,16,17,40,44] There are several other comparable general purpose systems used in medical physics such as the ITS (Refs. 54 and 55) and MCNP systems[11,32] both of which have incorporated the electron transport algorithms from ETRAN (Refs. 10 and 56) which was developed at NIST by Berger and Seltzer following the condensed history techniques proposed by Berger.[9] Other newer general purpose systems include PENELOPE (Ref. 34) and GEANT4.[33] The EGS and ITS/ETRAN and MCNP systems are roughly of the same efficiency for calculations in very simple geometries when no variance reduction techniques are used, whereas the other systems tend to be considerably slower. An important special purpose code is the EGS user code, BEAM.[23,57–60] The BEAM code is optimized to simulate the treatment head of radiotherapy accelerators and includes a number of variance reduction techniques to enhance the efficiency of the simulation.[46] Comprehensive reviews of MC simulation of radiotherapy beams from linear accelerators are available elsewhere.[24,25]

While the accuracy of these general-purpose codes can be roughly the same as long as they are carefully used, these codes are considered too slow for routine treatment planning purposes. Several groups have published on the use of parallelization of MC techniques over multiple computers to provide more reasonable turn-around times for simulation in clinical research.[61–63] Specific to radiation therapy, there have been a variety of MC codes developed to improve the calculation efficiency, especially in the patient simulation. The PEREGRINE system (North American Scientific: Nomos Division) was developed at the Lawrence Livermore National Laboratory and has been benchmarked against measurements.[27] The PEREGRINE electron transport algorithm is a modified version of the EGS4 condensed history implementation. PEREGRINE uses the random hinge approach[64] for electron transport mechanics. Several efficiency enhancing and variance reduction techniques are implemented in PEREGRINE, including source particle reuse, range rejection, Russian roulette and photon splitting. Parallelizing the calculation on several computer processors is also implemented to reduce the overall dose calculation time. The system decouples the scoring zones from the transport geometry. Source modeling in PEREGRINE is achieved by performing a full MC simulation of the accelerator head using the BEAM code[23] and using the output to create a source model[65] from which source particles are regenerated above the patient-dependent beam modifiers. PEREGRINE uses several approximations when transporting the beam through the patient specific beam modifiers, followed by transport through a patient's CT data set.[66] The PEREGRINE system was the first MC algorithm to receive FDA 510-K approval and represents the first commercially available photon beam treatment planning system in the United States.

Several commercial MC implementations currently available or under development are based on the Voxel Monte Carlo (VMC) series of codes. The initial version[37] of VMC was only applicable to electron beams and involved several approximations in the modeling of the underlying interaction processes. Improved treatment of multiple elastic scattering[67] was incorporated in 1996, PENELOPE's random hinge method in 1997,[68] and all remaining approximations removed in 2000.[45] A photon transport algorithm was added in 1998,[35] which included precalculated interaction densities in each voxel similar to approaches developed previously.[69,70] The resulting code was named XVMC. In 1999, a series of advanced variance reduction techniques were developed and incorporated into XVMC which brought an additional factor of 5–9 increase in simulation speed. Treatment planning applications and experimental verification of VMC-based systems have been reported in several articles.[71–75] Separate versions of the VMC code were subsequently developed by Fippel (XVMC) (Refs. 45 and 76 and Kawrakow (VMC++)[36]. XVMC is being incorporated into the Monaco (CMS), PrecisePlan (Elekta), and *i*Plan (BrainLab) treatment planning systems. VMC++ includes additional refinements in the physics models, such as the exact Kawrakow–Bielajew multiple scattering formalism,[77] including relativistic spin effects,[17] and the STOPS method (mentioned in Sec. II D). VMC++ is the basis for the first commercial electron MC algorithm from Nucletron and is being incorporated into the Masterplan (Nucletron) and Eclipse (Varian) treatment planning systems for photon beam dose calculations. The VMC/XVMC/

VMC++ code systems have also been integrated into several MC-based research systems including those at the University of Tubingen, McGill University, and the Virginia Commonwealth University.

Another MC code that has reached commercial implementation is the Macro Monte Carlo (MMC) method[38,78] for electron beam treatment planning. MMC uses the MC technique, but is very different from the standard simulation of radiation transport. MMC uses a precalculated database from EGSnrc simulations of electron transport through small spheres of varying sizes and materials and follows a random walk through the CT phantom based on these precalculated values. The commercial implementation of MMC, eMC, (Eclipse, Varian) makes use of some precalculated accelerator-specific information; however, fluence intensities arising from the various subsources are fitted to the user's measured data.[79] More details on the performance of the eMC system for clinical electron dose calculations is available elsewhere.[80]

There are several institutions currently engaged in developing MC radiotherapy applications for clinical and/or research related purposes. MCDOSE (Ref. 53 and 81) is among the first of these types of systems. MCDOSE is based on EGS4 and includes fundamental changes in some aspects of the electron transport in order to improve speed. MCDOSE has been shown to give results very similar to EGS4.[53] It performs particle tracking through the beam modifiers in conjunction with the patient calculation and has built-in capability to handle various models of the incident beam. The speed ups have been obtained by using various techniques (bremsstrahlung splitting, photon forcing, track repetition,[37] and range rejection).

The MCV (Monte Carlo Vista) [82] code is used for clinical IMRT planning and verification[61] as well as for a variety of research related applications. MCV interfaces photon-electron MC dose algorithms to the Pinnacle (Philips Radiation Oncology Systems, Madison, WI) commercial planning system, and calculations are performed in a parallel environment using multiple Unix-based processors.[82] Treatment head simulation is accomplished using a modified version of the BEAM code, with calculations divided into two stages, based on the patient-dependent[83] and patient-independent component structures.[82] Patient and phantom calculations (within MCV) are completed using DOSXYZnrc,[58] VMC++ (described above), or MCVRTP, a C++ MC code developed by Philips that uses many of the algorithms of EGS4.[82] MCV utilizes variance reduction techniques inherent to the subcodes it uses, and achieves speed by use of multiple processors.[82]

Another major research code is the dose planning method[39] (DPM) code system developed initially for performing electron beam dose calculations in a voxelized geometry. DPM utilizes the Kawrakow–Bielajew multiple scattering formalism[77] and the random hinge approach for transport mechanics.[64] Particles do not stop at boundaries[39] as is the case with other fast codes. DPM has been integrated into the University of Michigan's in-house treatment planning system (UMPlan) and is currently being used for a variety of photon beam treatment planning studies.[84,85]

An MCNP (Monte Carlo *N*-particle)-based code, RT_MCNP (Ref. 86) has been in use for treatment planning research at UCLA. There have been a series of publications related to the use of RT_MCNP for a variety of applications, from radiosurgery to IMRT planning using a micromultileaf collimator.[86–91] Finally, treatment planning studies using the GEANT,[92–94] PENELOPE,[95] gamma electron positron transport system (GEPTS),[96,97] and ORANGE (Ref. 98) (MCNP-based) MC codes have also been reported.

In an effort to quantify the speed and accuracy for the phantom component of the calculations by the various MC codes being used for research and/or clinical planning purposes, Rogers and Mohan[99] proposed what came to be known as the ICCR benchmark. The tests and geometries for the ICCR benchmark comparisons were as follows:[99] (a) speed test: phantom of dimensions $30.5\times30.5\times30$ cm with $(5\ \text{mm})^3$ voxels filled either randomly with one of 4 materials (water, aluminum, lung, and graphite) or with water alone, 6 MV photons (spectrum) from a point source at 100 cm SSD and collimated to 10×10 cm^2 at the phantom surface, (b) accuracy test: heterogeneous phantom as defined in (a) with $5\times5\times2$ mm voxels (2 mm along the depth axis), 18 MV photons (spectrum) from a point source at 100 cm SSD and collimated to 1.5×1.5 cm^2 at the phantom surface. Beam spectra[268] were provided for these comparisons in order to standardize the beam model used in the dose calculations. Statistical uncertainties were to be reported as the relative uncertainty in the dose for voxels with a dose greater than some arbitrary lower limit, such as 50% of the maximum dose.[99] Results for the ICCR benchmark are summarized in Table I. Some timing results have been added recently. Timing values have been scaled to that on a single Intel P-IV 3.0 GHz processor.

The reader should be aware that the timing results reported in Table I are susceptible to large variations (on the order of at least 20%) due to variations in compilers, memory size, cache, etc.[99] Timing comparisons for more clinically relevant treatment plans are presented in Sec. III E 4. These results have been reported by medical physicists using commercial MC systems for treatment planning.

III.B. Accelerator treatment head simulation

III.B.1. Sensitivity of simulations to electron beam and other parameters

In general one does not know all the details of the clinical accelerator. For example, the characteristics of the incident electron beam are only known approximately. Knowledge of the sensitivity of MC simulation results to input parameters, such as the position, direction, and energy of the initial electron beam exiting the accelerator and to details of the geometry of the treatment head, is important. A sensitivity analysis is indispensable in determining which source and geometry parameters to adjust and by how much in order to improve agreement with user-specific measurements.

Factors influencing the characteristics of a photon beam are the energy, spatial, and angular distributions of the electrons incident on the target (or exiting the waveguide), and

TABLE I. Summary of timing and accuracy results from the ICCR benchmark. Timing comparisons were performed using 6 MV photons, 10×10 cm^2 field size, and those for the accuracy test, using 18 MV photons and a 1.5×1.5 cm^2 field size, as detailed in the ICCR benchmark (Ref. 99). All times have been scaled to the time it would take running on a single, Pentium IV, 3 GHz processor. Readers should be aware that the timing results, as well as the method used to scale the times, are subject to large uncertainties due to differences in compilers, memory size, cache size, etc.

Monte Carlo code	Time estimate (min)	% mean difference relative to ESG4/PRESTA/DOSXYZ
ESG4/PRESTA/DOSXYZ	43	0, benchmark calculation
VMC++	0.9	±1
XVMC	1.1[a]	±1
MCDOSE (modified ESG4/PRESTA)	1.6	±1
MCV (modified ESG4/PRESTA)	22	±1
DPM (modified DPM)	7.3[b]	±1
MCNPX	60[c]	Maximum difference of 8% at Al/lung interface (on average ±1% agreement)
PEREGRINE	43[d]	±1
GEANT4 (4.6.1)	193[e]	±1 for homogeneous water and water/air interfaces

[a]Results not originally part of the ICCR benchmark study, from Ref. 76.
[b]Results not originally part of the ICCR benchmark study, reported independently by author I.J.C. for the modified version of DPM developed for clinical planning calculations.
[c]Timing results not originally part of the ICCR benchmark study, reported independently by author J.J.D. Calculations were performed using the *F8 (energy deposition) tally.
[d]Timing and accuracy results not originally part of the ICCR benchmark study, reported independently by author D.S.-B.
[e]Timing and accuracy results not originally part of the ICCR benchmark study. Estimated independently by author Seuntjens based on Poon and Verhaegen (Ref. 94) and ICCR type speed-test dose calculations (Ref. 270). Timing results are for the standard physics model; the low-energy and the PENELOPE model lead to a factor of 2 more CPU time. The accuracy result reported is derived from the interface perturbation studies in Poon and Verhaegen (Ref. 94), applies to 1.25 MeV monoenergetic photon beams and represents the difference with EGSnrc using PRESTA-II electron step algorithm and "exact" boundary crossing. For a water/Pb interface and 1.25 MeV photons, the maximum difference with EGSnrc increases to 6% (Ref. 94).

the dimensions, materials, and densities of all the components interacting with the beam (the target, primary collimator, flattening filter(s), monitor chamber, collimating devices, such as blocks or MLCs, and beam modifying devices such as wedges). Several investigators have reported on the sensitivity of megavoltage beam simulations to the electron beam striking the target and other treatment head parameters.[19,100–103] Faddegon *et al.*,[19] in simulating Siemens accelerators, showed that the key parameters are the mean energy and focal spot size of the electron beam incident on the exit window, the material composition and thickness profile of the exit window, target, flattening filter, primary collimator, and the position of the primary collimator relative to the target. Bieda *et al.*[101] showed that the accelerator simulation for 20 MeV (Varian-produced) electron beams was very sensitive to the distance between the scattering foils and, to a lesser extent, to the width of the shaped secondary scattering foil. Changes to the primary or secondary foil thickness were found to significantly alter the falloff and bremsstrahlung components of the depth-dose curve.[101] Sheikh-Bagheri and Rogers[102] performed calculations of "in-air" off-axis ratios and depth-dose curves and compared these with measurements to derive estimates for the parameters of the electron beam incident on the target, and to study the effects of some mechanical parameters, such as target width, primary collimator opening, flattening filter material, and density. Their study[102] included several different photon beam energies from accelerators produced by different manufacturers (Varian, Siemens, and Elekta). The electron beam radial intensity distribution was found to influence the off-axis ratios to a great extent. The greater the width of the electron-beam radial intensity distribution, the relatively more intense is the photon beam on the central axis.[102] Figure 3 shows the influence of the electron-on-target energy and radial intensity FWHM on 40×40 cm^2 field profile doses from Tzedakis *et al.*[103] The calculated profiles are observed to be quite sensitive to these parameters. The central axis depth dose curves are also strongly influenced by the electron-on-target energy.[102] However, the central-axis depth-dose curves are quite insensitive to variation in the radial intensity distribution of the electron beam striking the target, because the dose along the central axis is deposited primarily by particles in the vicinity of the central axis. The divergence of the electron beam incident on the target also needs to be considered as it may affect large field profiles.

Regarding the influence of individual treatment head components, Sheikh–Bagheri and Rogers[102] (see Table II) showed that even small changes (0.01 cm) in the primary collimator's upstream opening can affect in-air off-axis ratios by restricting the number of bremsstrahlung photons contributing to the scattered photon fluence reaching off-axis points downstream. Dose profiles are quite sensitive to the composition and density of the flattening filter as noted in Fig. 4, where two different flattening filter materials were used for

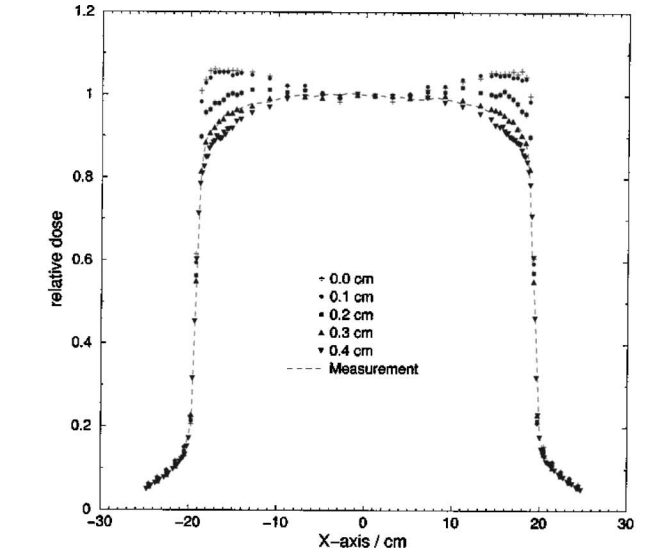

(a)

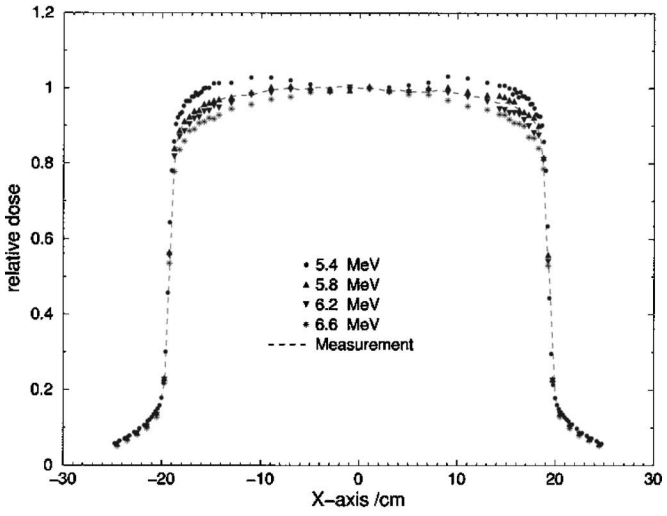

(b)

FIG. 3. (a) The lateral dose-profile curves as a function of the FWHM of the radial intensity distribution for a monoenergetic, 6 MV, electron beam. The measured profile and five calculated dose profile curves are presented; each curve is normalized to the central axis. (b) The influence of electron energy on dose-profile curves. The energy was varied from monoenergetic 5.4 to 6.6 MeV. For clarity only four calculated and measured profiles are presented; each curve is normalized to the central axis. The FWHM of the radial intensity distribution was 0.3 cm FWHM in all cases. Reprinted from Tzedakis *et al.* (Ref. 103) with permission.

the calculations.[102,104] The careful specification of the geometry and materials within the MC code is an important consideration. This includes verification of the input of the component geometric specifications, for example, by using the listing files available with the BEAM (Ref. 23) system. Moreover, for complicated components, such as the flattening filter, independent attenuation calculations of these structures, using monoenergetic photons, may be helpful to verify their thickness profiles.[105,106] Attenuation of the photon beam by the monitor ion chamber and the field mirror is negligible and these structures are often omitted from MC simulations of photon beams, except when backscatter to the monitor chamber is being taken into account. The ion chamber and mirror are, however, potentially important structures in electron beam simulations. The collimating jaws have no significant effect on the energy and angular photon distributions.[14,107,108] Changing the composition of the secondary collimators from pure tungsten to an alloy containing 50% tungsten by weight does not significantly affect the calculated dose.[102]

Even in those cases for which the beam model includes an explicit simulation of the accelerator head, end users of MC treatment planning algorithms will probably have little control over parameters affecting the treatment head simulation. It will be incumbent upon vendors to provide accurate beam models (verified by measurements) for treatment planning purposes. Vendors and developers should be aware of potential difficulties associated with accurate specification of the treatment head component structures. Such issues include difficulty in obtaining proprietary information from accelerator manufacturers, incorrect proprietary information provided by the manufacturers,[101,102,104] undocumented accelerator updates, and large uncertainties in important parameters needed for accurate simulation, such as the electron-on-target energy. Accelerator vendors are encouraged to make accurate, detailed information of their accelerators accessible in formats easy to implement in MC simulation, as established for instance by Siemens.[109]

III.B.2. Electron beam specifics

Simulation of the passage of electron beams through the treatment heads of accelerators has figured prominently in MC radiotherapy calculations for many years. The first application of the BEAM code[23] was to simulate electron beams for a wide range of accelerators. A variety of publications have demonstrated the accuracy of this technique for computing dose distributions and output ratios.[24,110,111] Recent work has established the methodology to achieve high accuracy in matching calculated and measured dose distributions for even the largest fields, including asymmetries and the bremsstrahlung tail.[112]

The procedure for simulating the electron beam treatment head is quite similar to that of x rays. The components generally important for electron beam therapy treatment head simulations are shown in Table III. Photon beam components are also presented for comparison. For electrons, accelerators from the major vendors use a pair of scattering foils to flatten the beam with minimal bremsstrahlung contamination. A low-scatter monitor chamber may be employed and the mirror may be retracted from the beam. The jaw position is generally fixed for a given applicator and energy such that the relative output ratio depends only on the custom insert.

The critical parameters for electron beam simulation are different than those for x rays. Sensitivity analyses provide quantitative evidence of these differences.[100,101,113] Due to the sensitivity of the beam range to the primary electron energy (a 0.2 MeV change in electron energy corresponds with a 1 mm change in beam range), the incident electron energy is the primary tuning parameter for electron beam

TABLE II. A summary of the findings of Sheikh-Bagheri and Rogers (Ref. 102).

Parameter in the linac model	Impact on in-air off-axis factors	Impact on central-axis depth dose values
Mean energy of the incident electron intensity distribution (assumed Gaussian)	**Decrease with increasing primary electron energy**, e.g., -0.105 ± 0.007/MeV at 15 cm off-axis for a Siemens KD 6 MV beam. **A 0.2 MeV mean energy change produces an observable effect**.	**A 0.2 MeV change in mean energy causes an observable change** (2% or 3σ with 0.7% or 1σ dose uncertainty).
Gaussian width of the incident electron energy distribution	**Show little or no dependence**, e.g., widening of the FWHM from 0% to 20% resulted in no change, for a Siemens KD 6 MV beam. Asymmetrical energy distribution has a small effect, e.g., an asymmetric Gaussian with 14% FWHM on the LHS of the peak and 3% FWHM on the RHS of the peak causes a change of 2% for a Siemens KD 18 MV beam.	**Show weak dependence in the dose buildup region and at large depths**, e.g., an asymmetric Gaussian with 14% FWHM on the LHS of the peak and 3% FWHM on the RHS of the peak increases buildup dose by up to 1.5% for a Siemens KD 18 MV beam.
Gaussian width of the incident electron radial intensity distribution	**Decrease quadratically with increasing Gaussian width**, e.g., a change in FWHM from 0.01 to 0.15 cm leads to 7% decrease at 15 cm off-axis for a Varian 18 MV beam.	**Little or no observable effect** considering statistical uncertainties.
Divergence of the incident electron beam (at a given intensity distribution FWHM)	**Show little or no effect up to 0.5°**; at 1° show a decrease of 1% at 15 cm off axis at 100 cm SSD, for an 18 MV Varian beam.	**No observable effect up to a few degrees** considering statistical uncertainties (1% or 1σ).
Radius of the upstream opening of the primary collimator	**Sensitive to small changes**, e.g., varying the upstream opening by 0.01 cm produces a 1% change at 15 cm off-axis for a Varian 18 MV beam.	No observable effect.
Density and material of the flattening filter	**Show strong dependence**, e.g., reducing tungsten density by 1 g cm^{-3} causes a 6% reduction at 15 cm off axis for a Varian 15 MV beam. **Using the incorrect material has a very large effect**, primarily because of the density change.	Not reported.

simulations. However, electron distributions are very sensitive to all the materials in the beam, especially the scattering foils and may also be affected by the monitor chamber if it has thick walls. Hence, accurate geometric descriptions of all components in the beam path are required for the simulation of electron beams. Asymmetries are evident in electron dose distributions and parameters to adjust include angle of the incident beam and the lateral position of shaped scattering foils and the monitor chamber.

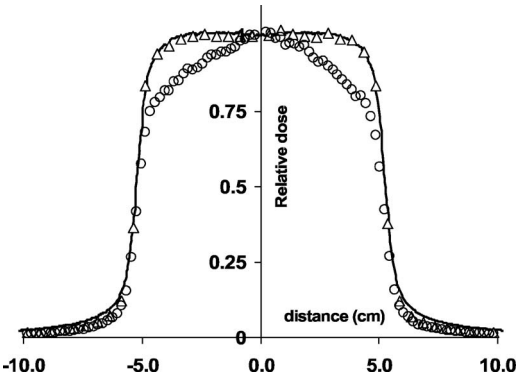

FIG. 4. MC calculated profiles in a water phantom (modified DPM, University of Michigan/UMPlan) for a 15 MV (10×10 cm^2) at 10 cm depth in water. Input for the profile calculations were the phase space simulations of the Varian 21-EX treatment head, performed using BEAMnrc, with two different material compositions specified for the flattening filter. Open circles represent the MC profile with a copper flattening filter ($\rho=8.933$ g/cm^3) and open triangles that with the tungsten filter ($\rho=19.30$ g/cm^3). Ion chamber measurements are shown in the solid line. Calculations and measurements are each normalized to the central axis (Ref. 104).

III.C. Modeling of the linear accelerator treatment head

III.C.1. General schemes

A beam model in the context of MC treatment planning is any algorithm that delivers the location, direction, and energy of particles to the patient dose-calculating algorithm. The direct MC simulation of a beam is one form of a beam model but for clarity we refer to it as a beam simulation rather than as a beam model. Accurate beam modeling is an important prerequisite for accurate dose calculation within the patient. Beam models use one of three possible ap-

TABLE III. Components in the treatment head and other beam modifying devices for x ray and electron beams.

X rays	Electrons
Exit window and target	Exit window and primary scattering foil
Primary collimator	Primary collimator
Flattening filter	Secondary scattering foil may be present
Monitor chamber	Monitor chamber (low scatter)
Mirror	Mirror
Asymmetric jaws and MLC	Jaw position fixed for each applicator
Wedge, blocks, graticule	Applicator with insert
Bolus	Bolus, shielding on or below patient surface

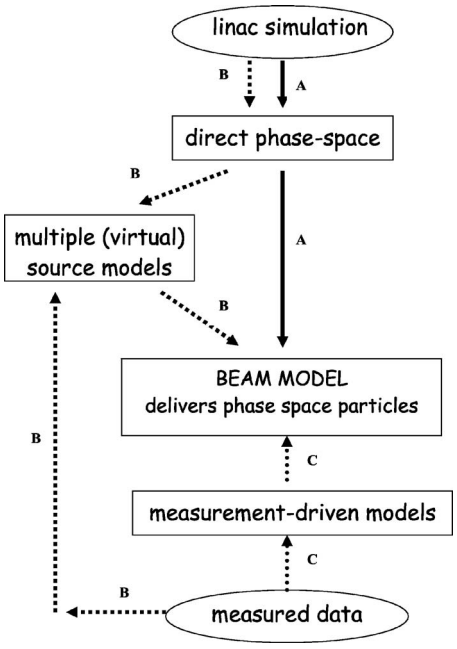

FIG. 5. The three "routes" for accelerator beam model specification: (a) solid line—direct use of phase-space information from simulation of the accelerator treatment head, (b) dashed line—multiple (virtual) source models derived from the phase-space information with or without enhancements from measured data, and (c) dotted line—development of other models derived from measurements (measurement-driven models).

proaches (see Fig. 5): (i) direct use of phase-space information from the accelerator treatment head simulation, (ii) development of virtual, multiple-source models reconstructed from the treatment head simulation with or without enhancement from measurements, or (iii) development of other models derived exclusively from measurements (measurement-driven models).

While the utilization of direct phase-space information provides details on the physical interactions within the treatment head, it may not be practical for routine clinical application.[65,93,114–116] Some of the limitations include: (a) generation and quality assurance of phase-space information requires MC simulation expertise, (b) accurate phase-space simulation is dependent upon accurate input parameters (such as the incident electron energy) as well as detailed geometric and material specifications of the accelerator components, which may be subject to inaccuracies, as well as proprietary issues, (c) storage requirements are large—typical MC simulation may require up to 10^9 phase-space particles for multiple photon beams,[115] which may amount to tens or hundreds of gigabytes of computer disk space for an accelerator with two photon energies and five electron energies with five different applicator sizes,[117] and (d) due to the much slower pace of speed increase in hard drives and networks compared to CPU speed development, reading the phase-space data can be a bottleneck in the calculation. It is therefore clear that a more concise, accurate characterization of radiation interactions in the treatment head is necessary for performing routine clinical MC dose calculation.

Another method for beam model specification, initially proposed by Ma *et al.*,[114] is based on the development of multiple-source models with parameters derived from the original simulated phase-space data.[65,88,93,114,116–120] In a multiple-source model, source particles are grouped by the location of their last interaction prior to being scored at the phase-space plane, resulting in subsources representing the major components of the treatment head. Fluence distributions for each subsource may be reconstructed from the phase-space data in the form of correlated histogram distributions,[65,93,114] thereby approximately retaining correlation of the particle's position, energy and direction. Although the development of accurate multiple-source models is also reliant upon simulation parameters and geometric and material specifications of the component structures, sub-sources may be "adjusted" (without redoing the simulations), based on measurements to optimize agreement between calculations and measured data, An example of such an approach consists of adjusting the spatial or energy boundaries of the planar fluence and energy distributions for each subsource to produce agreement with measured dose profiles and depth-dose curves, respectively, for a range of square field shapes, starting with fluence distributions reconstructed from phase-space data for one field size.[117,121] For instance, one changes the range of energies sampled from the discrete energy distribution as a function of radius, to provide a match with measurements, without having to redo the entire treatment head simulation. This method has been extended to MC-based commissioning of electron beams.[111,121] Models developed for reference accelerators were used to accurately commission (within 2%/2 mm of measurements in the high dose/high gradient profile regions) electron beams from other machines of similar design by adjusting a few parameters in the model. Implementation of photon and electron beam multiple-source models has been reported for a variety of accelerator manufacturers including, Varian,[122,123] Siemens,[73,124,125] Elekta,[73,86,88] Novalis (BrainLab),[87,89] and Cyberknife.[126]

A possibly more practical approach to beam modeling involves derivation of the model parameters from a standard set of measurements. The advantage of such measurement-driven models is that they may be developed without dependence on the details of the accelerator treatment head. Fluence distributions in measurement-driven models may be developed starting with analytical models whose parameters are optimized based on minimization of the differences between calculations and measurements.[100,125,127–131] Information for the model can be deconvolved from measured data.[100,127] Similar methods have been reported for beam-model specification using conventional dose calculation algorithms with good agreement established between calculations and measurements in water phantoms.[132–135] The same beam modeling criteria for conventional dose algorithms should also be applicable to the MC method although differences in the technical details such as source parameterization and software implementation are expected. The use of measurement-driven beam models eliminates the need for phase-space simulation and, as the model parameters are derived from measurements, may provide an added level of

confidence in the accuracy of the model in homogeneous phantoms. Moreover, specification of beam models is similar to that with conventional dose algorithms, and does not require expertise with MC accelerator simulation. However, rigorous verification of measurement-driven models in heterogeneous phantoms is necessary to validate the (empirically derived) fluence distributions. It has been shown that, in addition to the use of measurements in water phantoms, test cases in heterogeneous phantoms under conditions of electronic disequilibrium may be necessary to determine the correct energy spectrum unambiguously.[136]

III.C.2. Patient-specific beam modifiers

Transport through the patient-dependent components (such as the field-defining collimators and the MLC) may be classified into one of the following three schemes, which we will term: (a) explicit transport, (b) explicit-approximate transport, and (c) pseudo-explicit transport. In an explicit transport scheme, all particles (with appropriate energy cutoff values) are transported using MC techniques through the components; all details of the design geometry (such as rounded leaf ends, interleaf spacing, etc. for a MLC) should be included in the geometry modeling.[72,115,137] With explicit-approximate transport, approximations are employed in the MC photon/electron tracking scheme to improve the efficiency of the calculation.[83,87,138,139] An example is the approach of Siebers *et al.*,[83] in which only first Compton scattered photons are transported through the MLC. The method of Tyagi *et al.*[139] includes simulation through the detailed MLC geometry accounting for all Compton scattered photons, however, ignores the secondary electrons, i.e., assumes they deposit their energies locally. In a pseudo-explicit transport scheme, beam fluence distributions are reconstructed from the phase-space simulation to develop subsources for characterizing components, such as the field defining jaws,[93,120] electron applicators,[114] and the MLC.[88] Although the need for time-intensive, explicit transport is obviated with the use of multiple subsources, the ability to incorporate detailed geometric characteristics of components like the MLC may be difficult with this approach. Appropriate benchmarking must be performed by developers and vendors to evaluate the tradeoffs between speed and accuracy related to the use of various beam model approaches in MC-based modeling of patient-specific beam modifiers.

III.C.3. Output ratios

The output ratio (or relative output factor) is the ratio of dose per monitor unit in a phantom for an arbitrary field size to that for a reference collimator setting, the latter usually 10×10 cm^2 at a SAD (or SSD) of 100 cm for a depth of 10 cm for x-ray beams.[140] Output ratios over the range of clinically useful field sizes are heavily influenced by the amount of head scattered radiation impinging on the phantom.[140,141] Radiation generated by clinical accelerators can be characterized by a primary photon source generated through the bremsstrahlung process, and other extrafocal sources accounting for scattered photons arising primarily from the flattening filter and primary collimator, typically 3%–8% of the energy fluence in a 10×10 cm^2 field. The primary source is a narrow sharp source normally a few millimeters in diameter, while the extrafocal sources tend to be much broader, more diffuse and bell-shaped in nature.[142,143] The output ratio is affected by the size and geometry of these sources. The collimators (jaws and MLCs) block the extrafocal source when the field size is sufficiently small ($<3\times3$ cm^2) and for smaller fields the primary source starts being blocked by the collimators. The combination of extrafocal source and primary source cutoffs cause the output ratios to fall off sharply at small field sizes.[143,144] Accurate source modeling of small fields is especially important in IMRT planning where multiple, small field, off-axis segments are often used.[61,87,145] For medium sized fields (10×10 cm^2–20×20 cm^2), output ratios are more likely affected by the extrafocal sources as the collimators are large enough to expose the entire primary source, however, small enough to eclipse the extrafocal sources. In large fields, beyond 20×20 cm^2, the extrafocal sources are nearly completely exposed—the increase in output ratios in these situations is primarily a result of phantom scatter, lack of backscatter from the collimator jaws to the monitor chamber, and stray radiation from the treatment head.[146,147] Depending on the location of the jaws relative to the transmission chamber (which varies among the different linear accelerator types), radiation backscattered from the jaws into the chamber can also have an effect on the output ratios. Relative to large field sizes (40×40 cm^2), backscattered radiation increases by 2%–3% at small field sizes (3×3 cm^2) for 15 MV photons on a Varian (21EX) linear accelerator, for example. Studies for photon beam MC algorithms have shown calculated output ratios to be within 1.5% of measurements over a range of field sizes when accounting for backscattered radiation.[27,139,148,149] MC calculated electron beam output ratios (for field size-specific applicators) have also been reported to agree with measurements within 1%–2%.[26,110]

III.C.4. Dose buildup

There has been considerable discussion on discrepancies between MC calculations and measurements in the dose buildup region. Hartmann-Siantar *et al.*[27] observed MC dose deficits of up to 5 mm distance-to-agreement versus measurements and attributed these discrepancies to a source of electrons in the accelerator head not fully accounted for in the treatment head simulation with BEAM. It has been shown that arbitrarily increasing the electron contamination by a significant amount removes the discrepancy.[27,88,125] As the result of further investigation, Ding[150] concluded that the discrepancy could not be explained by the electron source hypothesis and postulated that contaminant neutrons emerging from the treatment head might be the cause. However, Ding *et al.*[151] subsequently refuted this neutron hypothesis by measuring minimal neutron component in the dose buildup region. Abdel-Rahman *et al.*,[152] who performed MC calculations (using EGSnrc) and a comprehensive set of measurements with multiple detectors, again found significant differ-

ences between measurements and calculations in the buildup region for 18 MV photons even when completely simulating the response of the detectors. They ruled out the following possible causes of the discrepancy: (a) an unknown electron source in the accelerator head simulation, (b) contaminating neutrons, (c) inaccurate cross section data, and (d) (gamma, p) reactions. They also showed that explicit modeling of triplet production interactions influences the dose buildup for an 18 MV beam. However, work by Kawrakow[153] showed that a more accurate triplet production model does not remove the discrepancies. Benchmarking of the NRCC accelerator photon beams has shown agreement well within 1%, for field sizes up to 10×10 cm^2, at all depths[154]; it should be noted that the NRCC accelerator (20 MV photons) uses a sweeping beam technique[154] as opposed to a flattening filter to flatten the beam. These comparisons explicitly accounted for stopping-power ratio variation with depth.

More recently, Kawrakow,[155] in performing detailed ion chamber simulations using the EGSnrc code system, showed that the relationship between measured ionization and dose for relative photon beam dosimetry depends on details of the chamber design, including cavity length, mass density of the wall material, size of the central electrode, and cavity radius, in addition to the beam quality and field size. When the correct ionization-to-dose relationship was used with the experimental data[155] and a variety of other improvements in the head simulations were made (e.g., using a larger diameter primary collimator opening and including the effects of extra shielding upstream of the jaws or MLC,[156] correcting a bug in the JAWS component of the BEAMnrc code, including an angular spread in the incident electron beam and several small effects in the simulation[153]), the discrepancies in the build-up region were reduced to an acceptable level. Chibani and Ma showed that resolving inaccuracies in the modeling of the primary collimator for a Varian 18 MV accelerator as well as including virtual sources for the lead shield and mirror frame, resulted in significantly better agreement between calculations and measurements in the dose buildup region.[156] Other sources of inaccuracy associated with detectors for dose buildup measurements are presented in Sec. III E 3.3.

III.D. Treatment planning: MC-based patient calculations

III.D.1. Statistical uncertainties

III.D.1.a. Latent variance and statistical estimators. For a finite number of independent simulated histories (N), the dose calculated using the MC method is subject to statistical uncertainty. By invoking the central limit theorem,[157] one can show that the statistical uncertainty in dose is proportional to $1/\sqrt{N}$, in the limit of infinite (large) N. There are generally two sources of statistical uncertainty in MC calculations of patient dose—those resulting from the simulation of the accelerator treatment head and those arising from fluctuations in the phantom/patient dose calculation. Sempau *et al.*[95] coined the term, "latent variance" to describe the uncertainty due to statistical fluctuations in the phase-space as opposed to the uncertainty due to the random nature of dose deposition in the phantom. Using an already calculated phase-space file, the statistical uncertainty in the dose calculated in a phantom by reusing the particles from the phase-space file (i.e., assuming they are independent and ignoring correlations between them), will approach the finite, latent variance associated with the phase space data, regardless of the number of times the phase space is reused. The use of source models derived from phase space simulation will tend to smooth out point fluctuations in the phase space.[114] However, if the latent variance is large enough to introduce systematic bias then this will be propagated in the reconstructed phase space (source model). Beam models derived exclusively from measurements, on the other hand, are analogous to those generated using conventional (analytical) algorithms—latent variance (as defined above) is not a concern for such models, but other systematic uncertainties in the beam model will be present. In estimating the statistical uncertainty in the patient dose calculation, it is necessary to account for the latent variance from the phase-space calculation as well as the random uncertainty from the patient calculation. To make this possible in practice, more work is needed to develop tools to assess the role of latent variance in patient dose calculations. Should latent variance be a significant factor in the total uncertainty, more independent phase-space particles need to be used in the patient simulations. It must be emphasized that all beam models are subject to systematic uncertainties, which are analogous to those introduced by the latent variance. For measurement-driven models, these uncertainties will be related to inaccuracies in the measurement data. Both types of models are subject to systematic uncertainties due to inadequacies in the model itself.

There are two common methods for calculating statistical uncertainties: the batch method and the history-by-history method. In the batch method, the estimate of uncertainty (standard error of the mean, $s_{\bar{x}}$) of a scored quantity, X, is given by

$$s_{\bar{x}} = \sqrt{\frac{\sum_{i=1}^{n} (X_i - \bar{X})^2}{n(n-1)}}, \tag{3a}$$

where n is the number of independent batches, X_i is the scored quantity (such as dose) in batch i, and $\bar{X}$ is the mean value of X over all the batches. The sample size is therefore given by the number of batches, where each batch is a calculation of the same quantity carried out with independent phase-space file inputs and random number sequences. In the history-by-history method, X_i represents the scored quantity in history i (rather than batch i) so that the standard error of the mean can be recast (in a mathematically equivalent form) as follows:

$$s_{\bar{x}} = \sqrt{\frac{1}{N-1}\left(\frac{\sum_{i=1}^{N} X_i^2}{N} - \left(\frac{\sum_{i=1}^{N} X_i}{N}\right)^2\right)}, \tag{3b}$$

where N is the number of primary (independent) histories, X_i the contribution to the scored quantity by independent his-

tory, i. An issue evident with the batch approach [Eq. (3a)] is that the sample size, n, is given by the number of batches. As n is usually small (on the order of ten or less) there is statistical fluctuation in the uncertainty itself. Advantages of the history-by-history method have been detailed elsewhere.[158]

An important consideration when calculating uncertainties is to take into account the correlation between a primary particle and all its secondaries, especially in the case of bremsstrahlung splitting where a large number of photons may all come from a single electron. Thus, to be strictly correct, these secondaries must be treated as part of the same history. If this correlation is not taken into account one can underestimate the uncertainty in a dose calculation, as the secondaries will be treated as independent particles thereby reducing the uncertainty erroneously. Another important case of correlation is when a single particle is being used several times as a source particle. In this situation it is important to recycle the particles, i.e., use them multiple times, all at once and treat them as part of the same history. If one were to restart the phase-space file multiple times, one would lose the correlation between particles which are all part of the same history. These secondaries would then be treated as independent particles causing the uncertainty to be underestimated. A more comprehensive review of the implications of recycling and restarting phase-space particles is provided in the paper by Walters *et al.*[158]

III.D.1.b. Influence of statistical uncertainties on dose distributions. For radiation therapy dose distributions, $s_{D_i} \propto \sqrt{D_i}$, where s_{D_i} is an estimate of the standard error of the mean (standard deviation/$\sqrt{N}$) of the dose in voxel i and D_i is the dose in that voxel.[159–161] The fractional (or relative) uncertainty in dose, $F_{D_i}=s_{D_i}/D_i \propto 1/\sqrt{D_i}$. In other words, the fractional uncertainty in dose in a voxel decreases as the dose increases. This relationship provides a useful rule of thumb when viewing dose distributions since it implies that the relative uncertainty in the dose in high-dose regions will be smaller than in low-dose regions, even though the absolute uncertainty is usually larger.

From Eq. (3b) we see that the uncertainty is roughly proportional to $1/\sqrt{N}$. Since, the simulation time $T \propto N$, it can be seen that achieving absolute precision ($s_D=0$) with MC simulation requires an infinite calculation time. Fortunately, absolute precision is not required in dose calculation results. This section concerns the precision required for MC simulation and the impact of a lack of precision on MC dose distribution quantities.

Radiation therapy dose distributions contain many voxels in which the dose is computed (for example, a cubic volume with sides of 10 cm contains 15 625 voxels with sides of 0.4 cm). Since the subvolume receiving a therapeutic dose can be highly variable, a standardized method to specify the statistical uncertainty for such a distribution is necessary. Although the statistical uncertainty can be specified for a single voxel in a dose distribution (such as that at the isocenter or at the maximum dose voxel, $D_{\max}$), as described below, these voxels are poor measures for the uncertainty of a MC computed plan. Alternatively, the statistical uncertainty over some volume, such as a planning target volume or some dose volume, such as the volume receiving greater than $X\%$ of the treatment dose, can be computed from the square root of the average variance of each constituent voxel. For example, the fractional uncertainty in the average dose for voxels with dose values greater than 50% of the maximum dose, $\bar{F}_{D>0.5D_{\max}}$ as suggested by Kawrakow, and Rogers and Mohan[99] could be used

$$\bar{F}_{D>0.5D_{\max}} = \sqrt{\frac{1}{K_{D>0.5D_{\max}}} \sum_{D>0.5D_{\max}} \left(\frac{\overline{s_{D_i}}}{D_i}\right)^2}, \tag{4}$$

where D_i is the dose estimate in the ith voxel, $\overline{s_{D_i}}$ is its uncertainty, and the summation runs over the K voxels with dose greater than 50% of $D_{\max}$. For clarity in communication, this report recommends that quantities, such as $\bar{F}_{D>0.5D_{\max}}$ or $\bar{F}_{\mathrm{PTV}}$ (or $\bar{F}_{\mathrm{PRV}}$) for doses to the specific volumes, planning target volume (PTV) or planning risk volume (PRV), be adopted as a standard method of reporting statistical uncertainties in dose averaged over the relevant volume. The use of uncertainties to voxels, such as the maximum dose should be avoided. In situations where doses in single voxels are important, such as the maximum dose to a "serial" organ like the spinal cord, users are reminded to also consider the statistical uncertainty of that dose voxel.[162] In such instances, it may be necessary to simulate a large enough number of histories so that s_{D_i} is very small.[162] This will ensure that the absolute uncertainty in the highest dose voxel will also be small. The statistical precision required for dose estimates in single voxels should be decided upon with guidance from the clinician. Users should also note that for a constant number of source particles, the statistical uncertainty also depends upon the size of the dose voxel. Reducing the volume to achieve a "point-like" voxel will require increasing the number of particles simulated to achieve constant statistical precision.

To varying degrees, statistical uncertainties affect all measures of the dose distribution, including output ratios, isodose profiles, dose-volume histograms, dose response parameters such as equivalent uniform dose and TCP/NTCP. In a uniform dose distribution, the dose metrics most sensitive to statistical uncertainties are the maximum and minimum dose voxels. These extreme values are by definition the voxels that have the greatest deviation from the mean dose. If one desires a region of uniform dose (e.g., within the PTV), that dose will not be uniform using a MC-based calculation, due to statistical fluctuations between adjacent dose voxels. The reported minimum and maximum dose voxels will differ from the mean of the idealized dose distribution by up to several standard deviations if many voxels are present in the distribution.[45,163] For example, in a uniform dose distribution with 15 625 voxels computed with MC algorithms, due to statistical fluctuations, there is a 63% probability that the dose in at least one voxel differs from the mean by more than four standard deviations.[45] With regard to dose prescriptions, the specification of the maximum dose to a single voxel when there is a desired volume of uniform dose (e.g., the

PTV), will result in an underdosage to this volume. Similarly, dose prescription to the minimum dose voxel will result in an overdose to the relevant volume. Isodose contours are also sensitive to statistical noise. For well-defined fields, such as rectangular fields used in beam commissioning, even 1% (1*s*) statistical uncertainty causes observable jitter in isodose contours. For patient fields that have irregular shapes, the acceptable amount of statistical uncertainty for isodose viewing is a matter of personal preference and should be agreed upon by the planner and the physician. It has been suggested that 2% statistical uncertainty on the D_{max} voxel is adequate for isodose evaluation.[160] When viewing statistical jitter in MC isodose distributions, the physicist should remind observers that overall dose delivery accuracy is limited to within a few percent; therefore there is uncertainty in the actual location of an isodose surface even when dose is computed with non-MC algorithms. From this point of view, the planning team can use MC isodose jitter as a mechanism to open the dialog on realistic dose uncertainty in actual treatment delivery.

Integrated dose quantities, such as dose volume histograms (DVHs) are less sensitive to statistical uncertainty.[159–165] DVHs computed with the MC method represent the actual DVH (that computed with a hypothetical 0% statistical uncertainty simulation), convolved with a statistical uncertainty distribution. With this realization, Sempau and Bielajew[159] and Jiang *et al.*[165] reported that the effect of the "statistical noise" on DVHs could be removed by deconvolving the uncertainty from the DVH, allowing substantial decrease in the required number of histories used, depending on the complexity of the DVH. In general, the blurring effect due to statistical noise is greatest for steep DVHs, such as those for PTVs, while shallow DVHs, such as those for critical structures are less affected.

The sensitivity of quantities such as TCP and NTCP to statistical noise depends upon the parameters used by the model[164] and on the magnitude of the noise. Kawrakow[161] has shown for general dose-based cost functions that the uncertainty in the cost function decreases more rapidly than the individual dose uncertainties when the plan is close to optimum as expressed by the cost function. This implies that during IMRT optimization, where plan updates are based upon evaluation of such cost functions, larger statistical uncertainty might be acceptable.

A method to reduce the effect of statistical uncertainties in MC dose distributions is to postprocess the dose distribution. These methods have been termed denoising or smoothing techniques. Various methods related to digital filtering,[166,167] wavelet thresholding,[168,169] adaptive anisotropic diffusion,[170] and denoising based on a minimization problem[171] have been proposed. A detailed comparison of these methods is presented in the article by El Naqa *et al.*[172] Denoising is an approximate, efficiency enhancing method (i.e., it is not a variance reduction technique) since it can introduce systematic bias into the calculation. Nonetheless, denoising techniques are useful as they can reduce the overall (systematic +random) uncertainty when the random component decreases more than the systematic component increases. Kawrakow presented a series of tests to evaluate the suitability of MC dose distribution denoising algorithms.[167] These tests are based on the fact that one can determine the "correct" dose distribution by simulating many histories (for a very high precision) and then comparing the denoised distribution from a simulation with a much smaller number of histories to the high precision results. The tests include:

- visual inspection of isodose contours,
- evaluating root-mean-square difference between dose distributions,
- evaluating the maximum dose difference,
- comparisons of dose-volume histograms with and without denoising, and
- comparing the fraction of voxels failing an $x\%/y$ mm test.

Denoising methods reduce the number of particles (and, hence, the calculation time) required to achieve a given uncertainty by a factor of 3–10. Denoising techniques require proper validation under the full range of clinical circumstances before they are used with MC dose algorithms.

III.D.2. Dose prescriptions and monitor unit calculation

The stochastic nature of the MC method raises questions for prescribing dose. It is common clinical practice to prescribe dose to a single voxel or to base the dose prescription on the maximum or minimum dose voxels. However, as discussed above (Sec. III D 1.2), in an approximately uniform dose distribution, the outliers (the maximum and minimum dose voxels) are subject to the largest statistical fluctuation and even other single voxel doses may lack the precision for monitor unit calculations. Standard treatment planning analysis methods using isodose distributions and dose-volume histograms rely on dose averaged over a volume. It is logical to extend this practice to the prescription of dose, thereby avoiding precision issues in doses calculated in small volumes. For example, dose may be prescribed to an isodose surface, to a region of uniform dose (averaged over many voxels) about the isocenter, or to a single point on a dose volume histogram. The practice is emerging to calibrate the calculated dose distribution by performing a calculation in the standard geometry where the accelerator is set to deliver a given dose per monitor unit, (e.g., 1 cGy/MU) at a given voxel. In this case, the dose at the calibration point may be calculated to high precision by averaging over a large number of voxels in a uniform dose region.

The issue of monitor unit calculations to specific single voxels within the target volume (e.g., the isocenter) for routine clinical planning may be confounded by large statistical fluctuations in the doses to individual voxels. Although the treatment planning practice is quickly moving toward volume-based dose prescriptions, particularly for IMRT planning, the ability to perform second MU checks for plan verification purposes is an important component of the standard practice. Until more efficient solutions are available, MU cal-

culations based on single-voxel-dose prescriptions should be performed with very high precision. That said, this task group encourages a shift in paradigm from point-based toward volume-based dose prescriptions, which we feel will soon become the standard method for prescribing doses in radiotherapy planning. The task group strongly discourages vendors from using the D_{max} or D_{min} dose voxels or other single voxel doses for dose prescription and monitor unit calculations in their MC-based treatment planning systems. Current users of MC algorithms are encouraged to find ways of circumventing point-based dose prescriptions if their systems are not flexible enough to allow otherwise. To obviate the concerns of dose prescription based on a single voxel, one institution (author J.E.C., Ottawa Hospital) has developed the following "work around" method for MC-based electron beam calculations: A dose distribution is calculated using 100 MU; this dose distribution in absolute terms is equivalent to a relative isodose distribution normalized to the standard calibration conditions (10×10 applicator, 100 cm SSD, d_{max} depth). For dose prescription, the physician chooses the isodose line that encompasses the target. The dose prescription point is then positioned on this isodose line along the central axis of the beam, and the treatment MUs are determined. A second calculation is performed as a check of the MUs and the final dose distribution.

For multiple 3D-CRT or IMRT fields, the procedure for generating monitor units is similar to that for single fields. For example, a given isodose line (such as the 95% line) can be selected for dose prescription and, for a given field, the dose contribution to a single voxel (e.g., the projected field cax point) along this line is determined from the treatment plan. For a calibrated MC algorithm, the absolute dose contribution from the given field in this voxel (on the selected isodose line) will be computed in units of cGy/MU, from which the monitor units for the beam can be calculated. A complete formalism for MU calculations for the different types of treatment deliveries has been provided by Ma *et al.*[173]

III.D.3. CT-to-material conversions

For conventional algorithms, electron densities extracted from the CT image are used to scale the influence of primary and, ideally, also secondary radiation interactions. MC algorithms utilize material density and the material atomic composition when performing particle transport. The differing atomic compositions of patient materials (e.g., soft tissue, bone, lung, air) result in different cross sections for the various radiation interactions. While material compositions cannot be determined solely from a single energy CT, they can be indirectly approximated by estimating the mass density from the electron density followed by assigning a material to each voxel.[37,86,174–176] For some MC codes, explicit material specification is circumvented by directly relating the CT [Hounsfield (HU)] numbers to material interaction coefficients, based upon parameterization of materials representative of the patient,[37] for example those tabulated in ICRU Report No. 46.[177]

To ensure proper correspondence between HU and materials (or material interaction coefficients), correspondence between these quantities must be established during the CT and treatment planning system commissioning process. To ensure appropriate material specifications, it may be desirable to have several conversion tables, whose selection is based upon knowledge of the particular patient's characteristics. Use of multiple calibration curves reduces the volume of inappropriate tissues specified in given regions, such as lung tissue within a prostate gland, however. Although the importance of exact material specification has been established in other studies,[178] more work in this area of research relevant to clinical treatment planning is necessary. Other information about the patient may also be helpful. For example, in a patient with a hip implant, it may be impossible to distinguish if the implant is titanium, steel, or a composite based solely on the CT numbers. In this case, material assignment based on knowledge of the material implanted in the patient would be beneficial. A recent evaluation of the influence of material compositions on dose distributions[178] showed dose errors of up to 10% for 6 and 15 MV photons, and 30% for 18 MeV electrons due to media and/or mass density misassignment, when comparing dose distributions between a known phantom and a CT-imaged phantom with compositions and densities assigned by a conversion process. The use of conversion techniques based purely on mass density (e.g., assuming the only patient material is water, but with varying density), as employed in conventional algorithms, is discouraged with MC simulation because most of these methods ignore dependencies of particle interactions on the materials, which can lead to notable discrepancies in high atomic number materials.[176]

CT number artifacts caused by issues such as beam hardening in the CT scanning process or by high density structures, such as dental fillings are potentially important in MC dose calculation. Other artifacts may arise, for example, when the CT scanner encounters a sharp edge, such as the surface of a rectangular solid phantom, where a blurred edge may result after image reconstruction. In one observed case, the resultant contour showed 3 mm of additional phantom, causing the MC-calculated percentage depth dose curves to be shifted 3 mm toward the surface.[269] Such issues are of relevance to both MC- and non-MC-based algorithms and will need to be taken into consideration in order to perform accurate dose calculations in the dose buildup region.

As with any dose algorithm, testing should be performed to evaluate the effect of artifacts on the accuracy of the MC dose calculation.[179,180] It must be emphasized that the accuracy of CT-number to material conversions affects all dose calculation algorithms, both MC- and non-MC-based methods.

III.D.4. Dose-to-water and dose-to-medium

Historically, radiotherapy dose measurements and calculations have been performed in, or specified in terms of the absorbed dose to water (D_w). With MC-based algorithms,

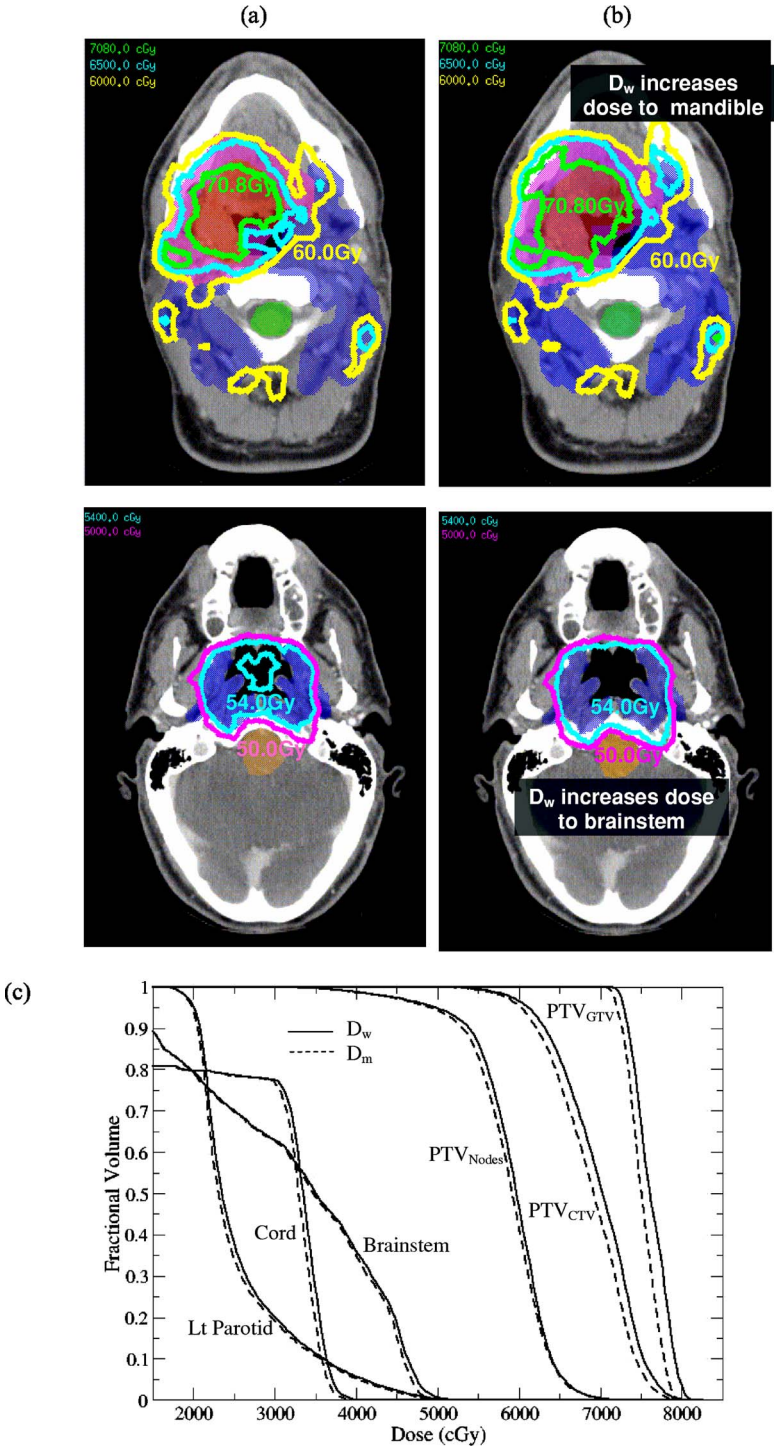

FIG. 6. MC-based (MCV system) dose-to-medium (D_m) and dose-to-water (D_w) results for a typical head and neck IMRT treatment plan: (a) D_m, (b) D_w, and (c) DVH comparison. Reprinted from Dogan *et al.* (Ref. 181) with permission.

particle transport simulations occur in materials representative of patient media; dose is therefore specified to the patient medium (D_m). For tissues with densities near 1.0 g/cm^3, the difference between D_w and D_m for megavoltage photon beams is small (1%–2%), however, for higher density materials, such as cortical bone, the difference can be as large as 15%,[176] since the stopping powers of water and these higher-density materials differ more significantly. Therefore, there is a systematic difference between the dose computed using conventional analytical algorithms and MC simulation. Figure 6 shows the dose and DVH differences between plans calculated with D_w and D_m for a typical head and neck IMRT treatment plan.[181]

To use MC simulation in the current clinical practice so as to be able to compare D_m with historical D_w results, requires a conversion of D_m to D_w for dose prescriptions, isodose coverage, dose-volume histograms, and any other dose related metrics. In this context, the converted D_w represents the dose to a small volume of water embedded in the actual medium. Whether one should eventually use D_m in place of

D_w directly in clinical prescriptions remains the subject of debate.[182] Arguments in favor of using D_w for dose specifications include:

- Historical clinical experience has been derived based on D_w, hence, D_w allows direct compliance with previous clinical experience and with conventional dose algorithms. Doses reported in clinical trials are based on D_w, hence, therapeutic and normal tissue tolerance doses are based on D_w.
- Accelerator and ionization chamber calibration protocols are D_w based.
- Tumor cells embedded within a medium are more water-like than medium-like, e.g., a tumor cell embedded in a bone matrix.

Arguments in favor of using D_m for dose specification include:

- D_m (or the dose to the tissues of interest) is the quantity inherently computed by MC dose algorithms. This may be of more clinical relevance than the doses on which historical clinical experience is based, which are approximate estimates of the true dose in the first place.
- Converting D_m back to D_w may involve additional complexity and introduce additional dose uncertainty.
- The difference between D_m and D_w for tissue equivalent materials is rather small and is likely to have minimal impact in clinical practice.
- It is known that, due to organ and target motion, the dose actually delivered in the course of a treatment may be significantly different from the planned dose. Conversion of Monte Carlo computed doses to D_w may analogously necessitate discussions on conversion to "dose to a static patient," should 4D planning and delivery techniques become routinely used in the clinic.[183]

The conversion of D_m to D_w or vice versa requires an application of Bragg–Gray cavity theory: $D_w = D_m(\bar{S}/\rho)^w_m$, where $(\bar{S}/\rho)^w_m$ is the unrestricted water-to-medium mass collision stopping power averaged over the energy spectra of primary electrons at the point of interest. One method to accomplish this conversion[176] is to utilize the fact that for patient-like materials, $(\bar{S}/\rho)^w_m$ is approximately invariant throughout a photon radiation therapy field (within 1%), hence, $(\bar{S}/\rho)^w_m$ can be used as a post-processing step to convert D_m to D_w. However, this requires that a sufficient number of materials be specified so that the material-dependent dose conversion approximates a continuous function.[184] Rather than postprocessing the dose conversion, one can multiply the energy deposited by primary and secondary electrons on each electron energy-loss step by the factor $(L/\rho)^w_m$, the ratio of the restricted mass collision stopping powers of water to local medium for the current energy of the electron. This is done in the MC transport code, thereby directly obtaining D_w. Alternatively, material interaction data may be evaluated over continuously parameterized space with cross sections and stopping powers for specific materials scaled relative to water.[35,37] Figure 7 shows a parameterization of the mass collision stopping power as a function of tissue density for different electron beam energies.[37] The fit is shown to be in good agreement with ICRU data[177] for body tissues. The advantage of this approach is that it circumvents the potential misassignment of media at material boundaries[37] which arises when the human tissue mass density range is divided into bins representing different tissues, especially when the number of material bins is small.[184]

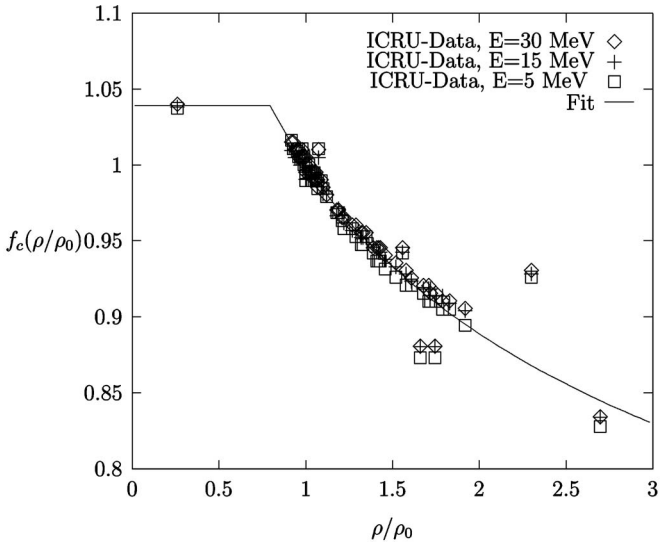

FIG. 7. Mass collision stopping power divided by the mass collision stopping power of water as a function of density normalized to water. A comparison of the fit function to the ICRU data (Ref. 177) for body tissues for electron energies of 5, 15, and 30 MeV is shown. The few points outside the curve are materials like urinary stones, which are considered to have negligible effects. Reprinted from Kawrakow *et al.* (Ref. 37) with permission.

Until further studies indicate clinical justification for selecting D_m or D_w, it is the consensus of this task group that MC dose results should: (a) explicitly indicate the material to which the dose is computed and (b) allow conversion between D_m and D_w using one of the methods discussed above, or other methods as developed in future investigations.

III.D.5. IMRT dose calculation and optimization

A strength of the MC method is its ability to accurately compute dose for complex dose delivery scenarios such as encountered in IMRT. IMRT often involves large intensity gradients and is usually delivered using a sequence of small static or dynamically shaped MLC segments. Under these circumstances, the assumptions used in conventional algorithms regarding scatter equilibrium and output ratio variation with field size often break down.[185] Additionally, in IMRT a significant fraction of dose to structures of interest (particularly dose limiting critical structures) is due to radiation scattered from or transmitted through the MLC.[186] MC simulation circumvents these limitations since it makes no assumptions regarding radiation equilibrium and can transport particles through the detailed MLC leaf geometry[87,137,187] to include MLC leakage radiation, even for dynamic MLC leaf sequences.[138,188,189]

In using MC calculation in IMRT, a consideration is the method used to incorporate the MLC into the dose calculation. Intensity modulation has been incorporated into MC simulation using the conventional planning system's intensity matrix,[190] independently generated fluence modification matrices,[87,92,191,192] or direct transport through the MLC.[61,189] Note that errors introduced by fluence approximations used during the MC dose calculation will be propagated through to the prediction of the patient's dose. Thus, when a fluence matrix approach is used for MC dose calculations, differences with respect to a conventional algorithm's heterogeneity correction will be detected, but fluence prediction errors may go undetected, particularly if the same fluence matrix is used both for the conventional and MC calculations. However, when MC simulation is used to transport directly through the detailed MLC geometry, these fluence errors should be detected. Accounting for geometric details in the MLC geometry, such as interleaf leakage is possible using a fluence matrix approach, however, will require a very high resolution calculation matrix, which may be a limiting factor. Moreover, the energies of the scattered particles through the MLC using such an approach will be approximate. Whether or not modeling the intricate details of the MLC (versus more approximate fluence matrix approaches) will lead to clinically significant differences in IMRT treatment planning is not a fully resolved issue. More treatment planning studies in this area of research are necessary to better understand the associated clinical implications.

Application of the MC method for IMRT QA has been demonstrated by several research groups[61,87,139,190,192–194] using MC simulation to recompute dose distributions optimized with the conventional dose planning algorithm. When using MC calculations as the reference plan and ignoring statistical fluctuations, dose differences between conventional and MC algorithms can be considered systematic.[195] Ma *et al.*[191] found dose errors in excess of 5% and 20% (relative to the prescribed dose) in targets and critical structures respectively due to patient heterogeneities, in comparing MC calculations (employing an independent fluence matrix) with a pencil-beam model. In comparing MC calculations with a conventional planning system's (pencil-beam model) intensity matrix for head and neck and lung cases, Wang *et al.*[190] found a 20% lower V_{95} (volume receiving at least 95% of the target dose) for a lung plan, and a 9% lower D_{95} (dose delivered to at least 95% of the target volume) for a head and neck plan. Average agreement among all head/neck and lung cases in this study, however, was quite good.[190] Regarding the transport of particles through the MLC, Siebers and Mohan[61] showed fluence-based IMRT dose underestimates of 4.5% in V_{95} and heterogeneity-based dose overestimates of 5% in V_{15} in the same treatment plan. In intercomparing MC codes, Reynaert *et al.*[196] reported deviations of up to 10% in DVHs between PEREGRINE and BEAMnrc calculations. These discrepancies were attributed to differences in modeling of the Elekta (SLi-plus) MLC, not caused by the particle transport in the patient. This study further illustrates the importance of careful modeling of the details of the MLC in IMRT treatment planning.

MC-based IMRT plan optimization is limited by the clinical availability of MC calculation as a whole and the large calculation time required to perform the multiple IMRT dose calculations required for optimization. MC simulation during optimization allows the optimizer to account for heterogeneity induced dose perturbations, as well as for MLC leakage and scattered radiation. Inaccurate dose algorithms used during optimization can result in convergence errors[195] in which the optimized fluence pattern differs from that corresponding to the optimal dose distribution.

Studies demonstrating the use of the MC method in IMRT optimization include the work of Laub *et al.*,[197] who utilized a MC algorithm to evaluate the cost function during optimization but a pencil beam to compute the cost function derivatives used by the optimizer. Jeraj *et al.*,[195] reported on convergence and systematic errors in the IMRT inverse planning process (for lung cancer) resulting from the use of convolution/superposition and pencil beam algorithms, versus the Monte Carlo method. A similar study for treatment planning of head and neck cancers was published by Dogan *et al.*[198] Another study by Siebers *et al.*[199] demonstrated the use of correction-based schemes to produce convergence of doses computed by conventional algorithms with MC calculations. Bergman *et al.*[200] reported on the use of an EGSnrc-based MC beamlet dose distribution matrix for IMRT planning using a direct aperture optimization algorithm. The goal of their work was to assess the improvement in accuracy over conventional algorithms in using MC methods for both the final dose calculation as well as in the inverse planning process.[200] Combining these methods with statistical smoothing and denoising techniques,[166–172] after comprehensive benchmarking, may allow introduction of MC-based IMRT optimization into routine clinical practice, particularly since it has been shown that cost functions converge faster than individual dose uncertainties.[161] For a review of other studies, the reader is referred to the article by Verhaegen and Seuntjens.[25]

III.D.6. Voxel size effects

As is the case with any dose calculation algorithm, calculated dose is affected by the size of the scoring voxel. For MC calculations, typical values in the scoring dimension are voxel sides of 2–5 mm for field sizes greater than 3×3 cm^2 and 1–2 mm for field sizes less than 3×3 cm^2. For calculations where geometric details of the MLC are included in the modeling, scoring voxel sizes no larger than 1–2 mm will be necessary to diminish volume averaging of dose from inter- and intraleaf leakage. As with conventional algorithms, MC-based IMRT calculations should be performed using voxel sizes of 2–3 mm or less in the high gradient regions.[201,202] In addition to affecting the spatial resolution, the statistical uncertainty will be influenced by the voxel size; reducing the voxel size will increase the relative uncertainty for a fixed number of source particles because fewer particles deposit dose in the smaller volume. Increasing the voxel size (and, hence, volume) will reduce the relative uncertainty but may introduce errors due to re-

duced spatial resolution. An example of the influence of volume-averaging effects resulting from the use of larger voxel sizes (~0.5 cm on each side) in MC electron calculations is discussed in Sec. III E 3.5.

III.D.7. Cross sections

The uncertainties in photon interaction cross section data in the energy range from 5 keV to a few MeV is of the order of 1%–2%.[203] Although many MC codes use the incoherent-scattering-factor approximation (which assumes scattering of photons from stationary, free electrons), this approximation is found to be accurate in the mega-voltage energy regime, where the energy of the incident photon is much higher than that of the electron *K*-shell binding energy.[204] An excellent review of the cross sections for bremsstrahlung production and electron-impact ionization has been provided by Seltzer.[205] It is shown that, in general, calculated cross sections for the various electron interaction processes are in agreement with measurements within the combined experimental and theoretical uncertainties.[205] It is felt that cross section and electron data in the megavoltage energy range are sufficiently accurate,[206] assuming that sampling of these cross sections is done accurately within a given code. These same effects will be present in doses computed with the convolution/superposition algorithm.

III.E. Experimental verification

III.E.1. Introduction

In this report experimental verification of the MC algorithm deals with how accurately the algorithm performs under different test conditions within a phantom. As with any algorithm, verification and testing is a necessary step to ensure safety of use in the clinical setting. It is the consensus of this task group that verification of a MC algorithm should be similar to that of any model-based dose calculation algorithm, such as convolution/superposition. The clinical commissioning and acceptance testing of dose calculation algorithms has been reported.[48–50] Additional testing to confirm the accuracy of the MC algorithm in situations of electronic disequilibrium will be helpful. Quantification of benchmark cases (such as the ICCR benchmark[99]) should be performed by either the user, or the vendor. The intent of this section is to provide some examples of additional types of testing that may be included to assure the accuracy of the MC algorithm. The specification of required measurements for acceptance testing and commissioning of the MC algorithm and the criteria for algorithmic agreement with measurements is beyond the scope of this report.

III.E.2. Previous work

Toward the goal of verification of dose calculation algorithms, there have been a variety of studies related to measurements in heterogeneous media. These investigations (see, for example, Refs. 207–212) have usually focused on establishing limitations of conventional dose algorithms in heterogeneous media and on how the use of physics-based algorithms, such as the convolution and MC methods, can be used to produce more accurate results. More recently, Arnfield *et al.*[213] found large differences (up to 10%) between collapsed cone convolution and MC (PEREGRINE) calculations in an 8 cm lung-equivalent slab embedded within solid water and irradiated by a 4×4 cm^2, 18 MV photon beam. Their work included film and ion chamber detectors and showed that MC calculations were in good agreement with measurements.[213]

With respect to patient planning, studies[91,115,214–219] have pointed out major differences between MC calculation and conventional methods, such as the 3D pencil beam and convolution/superposition algorithms. Over the past ten years, there has been a growing interest in the use of the MC method in clinical treatment applications with many institutions around the world actively involved in the development and testing of such systems. Many experiments in homogeneous and heterogeneous phantoms[26,27,71,75,82,84,86,93,96,115,119,194,213,220–225] have been directed toward verification of MC algorithms for clinical planning applications. The interested reader is referred to these and other related publications for a comprehensive review of the various types of experimental testing of MC treatment planning algorithms.

III.E.3. Types of verification experiments

Experimental verification of a MC algorithm should include testing to assess the accuracy of: (a) the beam model (be it measurement-driven or based on treatment head simulation) and (b) the radiation transport algorithm in homogeneous and heterogeneous phantoms. The former is part of routine commissioning of dose calculation algorithms, whereas the latter is likely to have significantly more involvement from developers and vendors.

III.E.3.a. The beam model. The purpose of verification of the beam (treatment head) model is to ensure that parameters, such as the incident beam energy (if used) are correctly "tuned" to produce dose distributions in agreement with measurement. Such verification is the same as that for any dose algorithm and may best be performed with measurements in a homogeneous (water) phantom. These tests should include the acquisition of depth and profile doses in a water phantom for a range of field sizes, as is routinely performed for conventional algorithmic verification, and documented in the AAPM TG-53 report.[48–50] In addition, the use of measured in-air off axis ratios may be useful for benchmarking the beam model. Calculated in-air off-axis ratios have been shown to be very sensitive to the incident electron beam parameters (e.g., mean energy, intensity distribution, etc.), as well as the dimensions and densities of other structures, such as the primary collimator and flattening filter.[102]

The multileaf collimator (MLC). Experiments to benchmark the MLC transport have ranged from arbitrarily shaped AP fields designed to verify overall penumbral and transmission dose[88] to more complicated MLC shapes designed to test modeling of detailed effects, such as transport through the rounded leaf ends,[83,87,226] tongue-and-groove

effect,[27,72,83,87,137] and intra/interleaf transmission.[27,72,83,87,137] The complexity of MLC verification experiments will depend on the usage of the MC algorithm in the clinical setting. For the purposes of 3D conformal radiotherapy (3D-CRT), the shaped field cases provided in Fig. A3–1 of the AAPM TG-53 (Ref. 48) report are good examples of tests designed to test overall MLC transmission and penumbral effects. In the context of 3D-CRT planning, the accurate modeling of details of the MLC and the influence of these effects on leaf transmission and penumbra may be of reduced clinical importance to the target doses (for an appropriate CTV-to-PTV margin) as these issues affect the dose at the field edges and outside the field.[227] For IMRT, it is now well established that the accurate modeling of MLC transmission and penumbra is critical.[61,227] A stringent test of the ability of the MLC model to accurately handle intra/interleaf transmission is presented in Fig. 8(a), for a Varian, Millenium 120-leaf MLC. In this example, the calculated MLC leakage radiation is compared with film measurements in a direction perpendicular to the leaf motion.[83] Figure 8(b) shows a comparison between MC calculations and film measurements for a MLC "picket fence" shape where the field is blocked by even numbered MLC leaves with odd numbered leaves retracted behind the jaws.[83] This test is useful in evaluating how accurately the tongue-and-groove effect is handled.

In designing a test suite for verification of the MLC transport accuracy, the clinical physicist should give special consideration to the detailed specifications of the MLC, particularly if the MC model is to be used for IMRT planning. These details include: density and composition of the MLC leaves, rounded leaf-end dimensions, intra/interleaf gaps, and tongue-and-groove dimensions. Discrepancies between MC calculations and measurements deemed significant by the physicist should be reported to the vendor; modification of the relevant parameters influencing the model accuracy, such as the MLC geometric model should be performed by the vendor to establish acceptable agreement between calculations and measurements.

Other beam modifying devices. The accuracy of MC simulation of beam modifying devices, such as wedges and blocks may be benchmarked using methods similar to that for conventional algorithms.[48] A publication on the experimental verification of the PEREGRINE MC system[27] included the acquisition of large wedged field profiles (40×20 cm^2) at various depths (see Fig. 13 of Hartmann-Siantar *et al.*[27]). The purpose of large field testing is to ensure that radiation transport through the wedge (or other beam modifying device) is in acceptable agreement with measurements across the entire physical range of the device. Unacceptable differences between calculations and measurements should be reported to the vendor—appropriate action should be taken by the vendor to help resolve these differences.

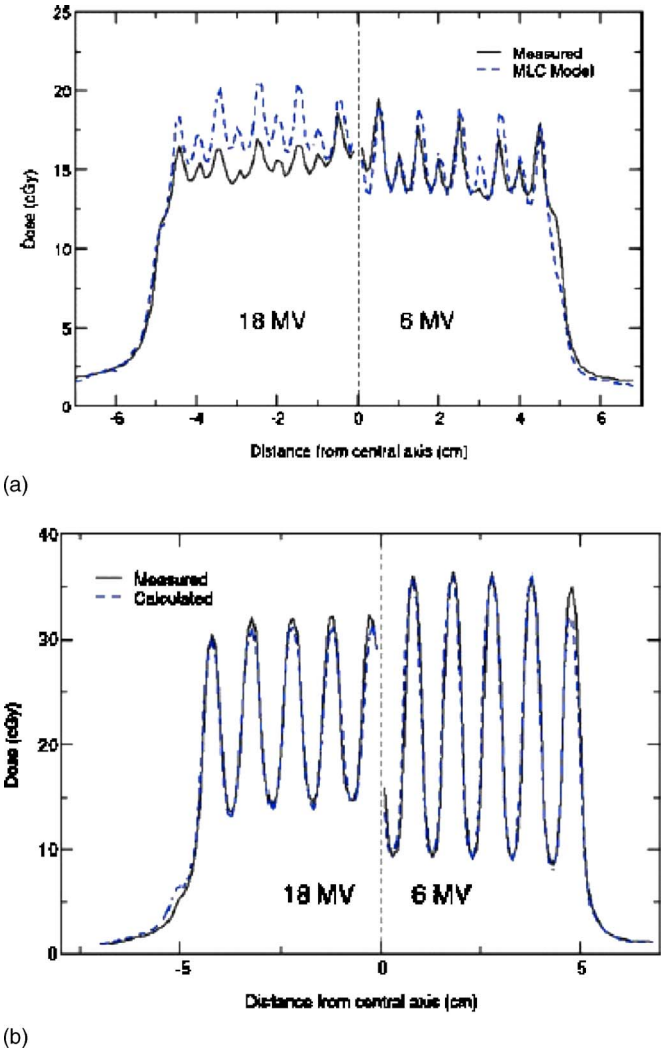

FIG. 8. (a) Measured (solid line) and calculated (dashed line) MLC leakage radiation perpendicular to the direction of MLC leaf motion for a 10×10 cm^2 MLC-blocked field for 6 and 18 MV beams. Dose calculation and measurement for the 6 MV beams occurred at 5 cm depth, 95 cm SSD, and the 18 MV data at 10 cm depth, 90 cm SSD. One should note that the dose due to leakage radiation (under the closed leafs) typically accounts for 2%–3% of the open field dose. The discrepancy noted for the 18 MV comparison is roughly 0.1% of the open field dose and is most likely to a small difference in the MLC density used in the calculations (Ref. 83). Reprinted from Siebers *et al.* (Ref. 83) with permission. (b) Measured (solid line) and calculated (dashed line) doses for 6 and 18 MV 10×10 cm^2 field (a) blocked by even numbered MLC leaves with odd numbered MLC leaves retracted behind the jaws. One should note that the dose due to leakage radiation (under the closed leafs) typically accounts for 2%–3% of the open field dose. Reprinted from Siebers *et al.* (Ref. 83) with permission.

III.E.4. Verification of the Monte Carlo transport algorithm in phantom

Given the improvement in the accuracy of MC simulation over conventional algorithms, particularly under circumstances of electronic disequilibrium, verification of the MC algorithm should include testing under these types of conditions to confirm the expected accuracy. Although reports, such as the AAPM TG-53 (Ref. 48) and others,[49,50] recommend testing in heterogeneous phantoms, issues related to electronic disequilibrium are generally excluded. This task group strongly encourages that verification testing of the MC algorithm include experiments emphasizing electronic disequilibrium effects, in addition to standard tests in heteroge-

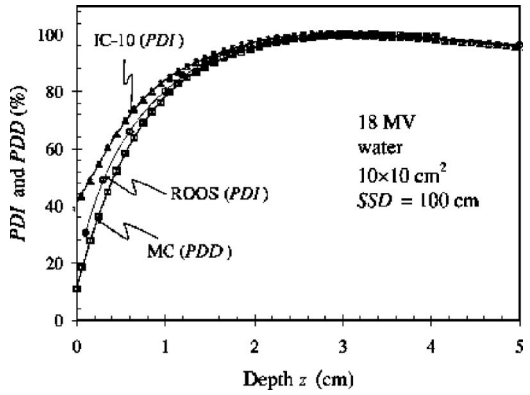

FIG. 9. Measured percent depth ionization and Monte Carlo calculated percent depth dose in the dose buildup region in water with the IC-10 cylindrical ionization chamber and the Roos parallel-plate ionization chamber in water for a 10×10 cm^2 field and SSD of 100 cm, for an 18 MV x-ray beam. For the IC-10 ion chamber, the effective point of measurement was 1.8 mm upstream from the chamber center. Reprinted from Abdel-Rahman *et al.* (Ref. 152) with permission.

neous phantoms as documented in other reports.[48–50] This type of testing is needed to exploit the advantages of MC-based simulation to its full potential.

Verification measurements in slab phantoms with embedded low density inserts and irradiated by high energy photons are useful in assessing the transport accuracy under conditions of electronic disequilibrium.[84,213,220] Effects of penumbral broadening of the dose distribution resulting from lateral electron transport may be evaluated using such phantoms.[84,213,220]

Dose measurements at various locations (depths and off-axis distances) both within and outside a high-density heterogeneity provide a benchmark to evaluate the perturbation of the photon and electron fluence due to the presence of the heterogeneity.[225] Dosimetric effects at interfaces (e.g., due to backscattering at bone/tissue interfaces[53,225]), transport within the heterogeneity, and the doses outside the heterogeneity may all be assessed with careful positioning of measurement devices within the heterogeneous phantom.

Experimental verification should also be performed in more clinically relevant situations. Examples of such geometries include thorax phantoms,[228] and mediastinal[229] and tumor-like phantoms.[229,230]

Verification experiments for algorithmic verification have also included the use of anthropomorphic (Rando) phantoms, where TLDs are most often used for the measurements.[225,231] With anthropomorphic phantoms, calculated patient treatment plans may be verified under a range of clinical circumstances. However, measurements must be carried out carefully with appropriate experimental techniques, theoretical interpretation, and reproducibility.

III.E.5. Dose buildup region

It is challenging to make accurate measurements in the dose buildup region. A recent study by Abdel-Rahman *et al.*[152] showed significant differences (see Fig. 9) in the dose buildup region (<1 cm) between the response of a parallel plate (Roos) and cylindrical ion chambers (IC-10, Scanditronix) in both 6 and 18 MV photon beams. Similar differences were found between a cylindrical ion chamber and a parallel plate chamber (P11) and a stereotactic diode (Scanditronix) by Yokoyama *et al.*[232] who measured dose buildup regions for IMRT fields. Based on the available literature, it is therefore recommended that dose buildups be carefully measured with either a parallel plate chamber, an extrapolation chamber, or with methods such as TLD extrapolation.[233] Diode detectors may also be considered for dose buildup measurements[234] but should be cross referenced with other detectors, such as parallel plate ion chambers. As pointed out by Kawrakow[155] (see Sec. III C 4), the relationship between the measured ionization and dose is sensitive to details of the ion chamber design and needs to be accounted for in dose buildup measurements.

III.E.6. Output ratios

MC calculations of output should be performed in a measurement-like geometry, usually consisting of a central axis point dose estimate at a fixed depth (d_{max}, 10 cm or other) in a water phantom for square field sizes defined by the collimating jaws. If the backscattered radiation into the monitor chamber is correctly modeled, it is possible to calculate output ratios to within 1%–2% agreement with measurements over a range of square field sizes, with sides from 3 to 40 cm.[146] In addition, comprehensive verification of output ratios should include testing for small segmental fields located off-axis, which are commonly used in IMRT planning. Output ratios should be verified against measurements of specially designed IMRT fields, such as junction narrow slit fields, in which the effects of small field dosimetry are magnified. Examples of such fields have been reported.[83,87,145,187]

III.E.7. Electron beams

Careful experimental verification is especially necessary for electrons because the tolerance of parameters, such as the electron energy and the treatment head structure constituents are much tighter than for photons. Accurate measurements are a prerequisite to accurate simulation. Care must be taken in measurement of the central axis depth-dose curve used to define the beam energy. Profiles in large fields need to be included to determine geometry details such as the distance between the scattering foils, the thickness of these foils, and the lateral position of shaped scattering foils, if present. Measurement of dose profiles in the bremsstrahlung tail are helpful to validate the photon component of the beam model.[112] Comparison to measured output ratios and dose distributions over the full clinical range of field sizes and SSDs is necessary for each applicator and beam energy, to rigorously validate the dose calculation. Further measurements, such as dose measured in an anthropomorphic phantom,[221] should be performed to validate the beam model for the specific MC-based application.

Comprehensive verification for electron beam MC simulation should include measurements in heterogeneous phan-

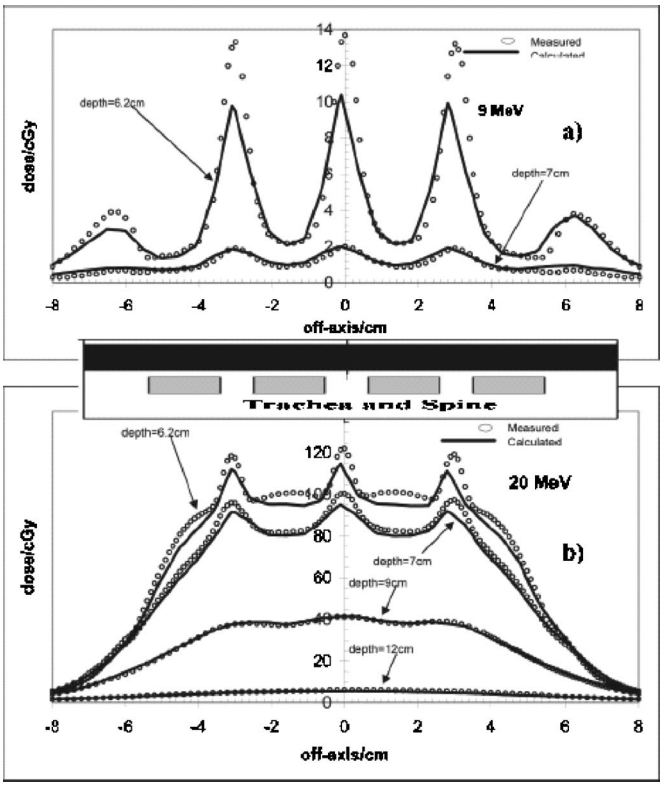

FIG. 10. Trachea and spine phantom: measured and Monte Carlo (Masterplan, Nucletron, based on VMC++) calculated crossplane dose profiles at various depths for: (a) 9 and (b) 20 MeV. SSD=100 cm, 10×10 cm^2 applicator. Monte Carlo simulations were performed with 50 000 histories/cm^2 and a voxel size of 0.49 cm. 100 MU were used for the calculations. The relative uncertainty in the calculations is about 1% – 1.5%. The phantom geometry is shown in the inset. Differences between measurements and calculations in this example were attributed to the volume averaging effects of a large voxel size (~0.5 cm) (Ref. 26). Reprinted from Cygler *et al.* (Ref. 26) with permission.

toms, such as those reported in the Electron Collaborative Working Group report[235] and its update.[236] Cygler *et al.*[26] performed experimental benchmarks using a variety of heterogeneous phantoms, including a 1D slab geometry with an aluminum slab insert, a 2D geometry with cortical bone-equivalent inserts ("ribs" geometry), a 3D cylindrical geometry with an "air" insert, and a complex trachea and spine equivalent geometry. Figure 10 shows the example trachea and spine phantom used in their study.[26] Differences between measurements and calculations in this example were shown to be due to the volume averaging effects of a large voxel size (~0.5 cm).[26] The MC calculations are found to underestimate the measurements because the large voxel size averages the density distribution in the vicinity of the heterogeneity, effectively reducing the calculated dose across the low-density heterogeneity.[26]

Careful measurements in such heterogeneous phantoms will provide rigorous benchmark data for verification of the MC algorithm, and as such should be strongly considered for testing purposes.

III.E.8. Measurement uncertainties

Making dose measurements is fraught with problems if the aim is to verify calculations at the 2% or better level, particularly in nonuniform dose regions. It is important to take into account point of measurement effects, variations in stopping power ratios for ion chambers, and beam quality dependence in general for other detectors (e.g., the well known over-response of film in regions of low mean photon energy), polarity effects, ion recombination effects, and chamber perturbation effects. Specific detectors may be required for accurate measurements under specific conditions; for example, properly constructed parallel plate chambers may be favored over ion chambers for measurements in the dose buildup region or at material interfaces. Uncertainties due to improper detector positioning must also be quantified as these measurements are often performed in regions of high dose gradients.

When using modern IMRT techniques there can be strong perturbation effects or corrections needed with ion chamber and other detector measurements. However, as with other algorithms, detector perturbations are generally not accounted for in verification of MC-based treatment planning algorithms. MC methods may be used to model the physical details of the detectors to provide a better understanding of measurements performed under nonequilibrium conditions. These approaches are available to developers of MC techniques but further advancement and investigation of this technology is necessary before specific recommendations can be made. Measurements form the basis for benchmarking the accuracy of dose calculation algorithms in clinical radiotherapy. It is therefore important that the uncertainties in the measuring techniques be accounted for.

III.E.9. Example experimental tests

Example tests for verification of MC dose algorithms are provided in Table IV. These tests, intended as a supplement to those provided in the AAPM TG 53 report,[48] aim to evaluate the various components of the MC algorithm.

III.E.10. Timing issues

The issue of calculation time is of considerable importance in the clinical treatment planning process. To provide a perspective on this subject, users of commercial MC dose algorithms were asked to submit calculation times for photon and electron treatment plans. The treatment plans ranged in complexity from simple AP beams to dynamically delivered IMRT plans. These results are summarized in Table V. As noted in Table V, photon beam calculations with PEREGRINE are approximately a factor of 2–3 times slower than those for conventional planning systems. However, these times will be reduced using faster, currently available processors (>2 GHz versus 800 MHz). Electron beam calculations with VMC++ (Nucletron) are roughly equivalent in processing times to conventional systems. The timing comparisons provide good justification of the fact that significant processing times are no longer a concern for routine clinical MC dose calculation. MC calculations for a plan with one beam take the same time as that for a plan with multiple beams (of approximately the same field size), for the same statistical uncertainty to the PTV. This is because the statistical uncer-

TABLE IV. Partial listing of example specific tests, phantom designs, and detector measurements for Monte Carlo treatment planning systems. These tests are intended as a supplement to those detailed in the AAPM TG-53 (Ref. 48) and other related publications (Refs. 49 and 50) for algorithmic verification. Note that extreme care should be taken when performing many of these measurements as they are, in some instances, highly sensitive to the measurement setup conditions.

Test description	Reason	Phantom design
• Water depth doses and profiles—emphasis on large open field sizes, ($>30\times30$ cm^2) • 2D planar dose perpendicular to the beam cax for large open fields	To evaluate the beam model accuracy—test is sensitive to structures like the flattening filter and other parameters, such as the electron-on-target energy.	• Depth doses and profiles at multiple depths measured in a water phantom using a cylindrical ion chamber.• 2D planar dose at multiple depths in solid water using film.
• 2D planar dose perpendicular to the beam cax of large MLC-shaped fields (see Fig. A3–1 of the AAPM TG 53 report)[a] • Dose profiles under the closed MLC leaves, perpendicular to the direction of motion (see Fig. 7).[b]	To evaluate the accuracy of the MLC model, leaf-tip penumbra and leaf transmission.	• 2D planar dose at multiple depths in solid water using film. • Dose profiles under closed MLC leaves measured with film or small volume detector (diode, TLD, pinpoint chamber, diamond detector).
• Small field (1×1 cm^2–4×4 cm^2) depth doses in low density media; larger field sizes should also be tested. • Penumbral broadening; lateral dose spreading in lung assessed over a range of field sizes (2×2–30×30 cm^2).	To evaluate the transport algorithm accuracy—use of high energies (>10 MV) and low density media emphasizes electronic disequilibrium effects.	• Depth doses in a layered phantom (see Fig. 8 and Fig. 1 of Rice *et al.*)[c] consisting of solid water and low density material (lung equivalent or cork) measured with small volume detector (diode, TLD, pinpoint chamber, diamond detector, at multiple point depths) or with film. Beam is directed perpendicularly to the slabs. • 2D penumbral measurements with film in planes perpendicular to the beam cax at depths above, below, and within the low density slab in the layered phantom. Beam should also be directed parallel to the slabs to evaluate interface effects.[d]
• Depth doses in high density media over a range of field sizes, 3×3–30×30 cm^2.	To evaluate the transport algorithm accuracy in high density media, such as cortical-bone equivalent slabs.	• Depth doses in a layered phantom consisting of solid water and high density material (cortical bone equivalent) measured with small volume detector (diode, TLD, pinpoint chamber, diamond detector) for smaller field sizes, or with film.
• Point doses in the vicinity of tissue interfaces (tissue/lung and tissue/bone), over a range of field sizes, 3×3 –30×30 cm^2.	To evaluate the algorithmic accuracy in the perturbed dose field at tissue interfaces.	See, for example, Fig. 1 of Ref. 230. Dose measured with film or with small volume detector, where possible, at incremental depths, for example, 0.2, 0.5, 1.0, 2.0, and 5.0 cm anterior/posterior to the medial and proximal tissue/lung equivalent and tissue/bone-equivalent interfaces.
• Dose evaluation in clinical treatment planning, for simple, intermediate and complex static treatment plans as well as IMRT plans, in anthropomorphic phantoms.	To assess the accuracy of dose calculation to points located within structures of different densities and receiving different doses based on the treatment plan.	• Dose measured with small volume detectors within inserts of different materials, ranging from air to cortical bone-equivalent. Plans designed should include simple, intermediate, complex static and IMRT beam arrangements. Anthropomorphic phantoms should be CT-imaged for planning purposes.

[a]See Ref. 48.
[b]See Ref. 83.
[c]See Ref. 229.
[d]See Ref. 222.

tainty is determined by the number of particles passing through a volume, and this number can be held constant when performing a MC plan with multiple beams. This is a distinct advantage over conventional algorithms where computational time scales linearly with the number of beams.

IV. CLINICAL IMPLICATIONS OF MONTE CARLO-CALCULATED DOSE DISTRIBUTIONS

IV.A. Introduction

In spite of our confidence in the improved dose calculation accuracy with a suitably commissioned clinical MC algorithm, we are confronted with the following clinical question: What is the effect of more accurate MC dose distributions on patient clinical outcome? To answer this question, we will need to investigate the correlation of MC calculated dose distributions with clinical outcome (in terms of tumor control and normal tissue toxicity).

To date the evidence directly correlating the improved accuracy of MC-calculated dose distributions with clinical outcome is scant. Investigations by De Jaeger *et al.*,[237] (which included convolution but not MC calculations), Chetty *et al.*,[238] and Lindsay *et al.*[239] are among the first

TABLE V. Summary of timing results for clinical treatment plans from currently available commercial Monte Carlo systems. Data for photon beams were provided by author G.E., performed using the PEREGRINE (Nomos division, North American Scientific) system and those for electrons by author J.E.C., conducted with Nucletron. The (1σ) relative statistical uncertainty was approximately 2% in the maximum dose voxel for the Nomos calculations and roughly 1%–1.5% (in the average depth dose along the central axis) for the Nucletron electron beam calculations. Eclipse calculations were reported with an uncertainty of 1%–2% in the mean dose of all voxels receiving more than 50% of the maximum dose within the body of the contour. Readers should be cautioned that the timing results are subject to large uncertainties due to differences in compilers, memory size, cache size, etc.

Monte Carlo code/configuration	Description of treatment plan	Time estimate (min)
PEREGRINE (Nomos, North American Scientific) 16 processors (8-dual), Pentium III, 800 MHz	AP beam, 6 MV photons, 10×10 cm^2 in a water phantom, cubic voxels with 2 mm sides	48
	5 field, 6 MV CRT prostate plan, $\sim7\times11$ cm^2, cubic voxels with ~2.4 mm sides	89
	5 field, 6 MV prostate plan with modulation delivered with DMLC (exposed field $\sim4\times8$ cm^2), cubic voxels with ~2.4 mm sides	71
Masterplan (VMC++, Nucletron), single CPU Pentium IV XEON, 2.2 GHz	AP beam, 6 MeV electrons, 10×10 cm applicator, water phantom, cubic voxels with 4.9 mm sides	4.2
	AP beam, 17 MeV electrons, 10×10 cm applicator, water phantom, cubic voxels with 4.9 mm sides	8.2
	AP beam, 20 MeV electrons, 15×15 cm applicator, water phantom, cubic voxels with 3.9 mm sides	21
	Breast boost treatment plan: 2 fields, 11 MeV electrons, $\sim3\times3$ cm cutouts, cubic voxels with 5.4 mm sides	8.6 (both fields)
eMC (MMC, Eclipse, Varian) single CPU Pentium IV XEON, 2.4 GHz	AP beam, 6, 12, 18 MeV electrons, 10×10 cm applicator, water phantom, cubic voxels with 5.0 mm sides	$\sim$3, 4, 4 (6, 12, 18 MeV, respectively)

studies evaluating the influence of improved dose distributions on outcome observed in patients treated with lung cancer. The study by De Jaeger *et al.*,[237] in which lung cancer treatment plans were retrospectively recalculated using a convolution/superposition (CS)-based algorithm (initially calculated with an equivalent-path-length (EPL) algorithm), showed clinically significant differences between calculated and observed incidences of radiation pneumonitis. They demonstrated that the calculated incidence of radiation pneumonitis correlated better with observed incidence when using dose distributions calculated with CS rather than EPL algorithms.[237] Although this study was carried out using a CS algorithm, it provides strong support that the dose-response relationships determined with correction-based algorithms will be different than those computed with model-based methods.[237] With the sometimes large differences observed between the doses calculated with CS and MC algorithms,[240] the MC method is likely to add a higher degree of accuracy to the dose-effect relationships, and will be instrumental in putting these relationships on a more solid footing.

There is clearly a need for more studies addressing the clinical impact of MC-calculated dose distributions. The use of retrospective data may provide a useful means to perform such studies. Retrospective dose assessments of already existing local tumor control and normal tissue complications, using doses recalculated with MC algorithms, may give an early indication of the clinical utility of the MC method, and may also help physicians determine how to use the new MC-calculated doses.[206] Retrospective analyses should eventually show us how to make use of this information in a prospective way.[206]

IV.B. Clinical examples

In reviewing the literature on clinical treatment planning, one should keep in mind that the dose differences found between MC-based and conventional algorithms will be highly dependent on the beam arrangements, field sizes, beam energies, tumor size, and location. This is particularly true in anatomical sites where the target is situated near tissues with widely varying densities, such as the lung and head/neck. For example, due to electron transport issues, differences found in a lung CRT treatment plan using small field sizes and 15 MV photons may be much larger than those found with a standard AP/PA lung plan, using large field sizes and 6 MV photon beams. The reader should therefore be advised that, although there is a general consensus on the importance of the MC method in sites such as the lung, the dosimetry in many of the reported studies is based on specific conditions. The following literature review will focus on treatment planning in the lung and head and neck since differences between MC-based and conventional algorithms are likely to be smaller in other external beam treatment sites. This does not include the potential for improvement in dose estimates in any site from accurate simulation of beam modifiers, in particular, the MLC for delivering IMRT. More studies using MC-based dose calculation techniques in clinical treatment planning are warranted to better quantify the dosimetric and clinical benefits of these algorithms.

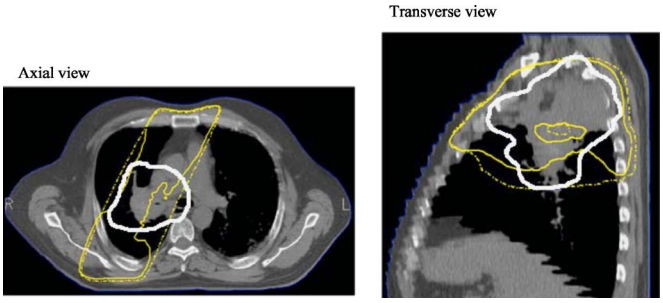

FIG. 11. Opposed, oblique field treatment plan (15 MV photons) showing the 100% isodose coverage for MC (modified DPM, University of Michigan/UMPlan) in the solid line, and an equivalent path length (EPL, University of Michigan/UMPlan) algorithm in the dashed line. The PTV is demarcated in white.

An excellent review of MC-based dose calculation methods in clinical planning for various treatment sites, including the breast and prostate is provided in the article by Reynaert *et al.*[241]

IV.B.1. Photon beam treatment planning

IV.B.1.a. Lung Perhaps the strongest motivation for the need for MC dose calculation comes from treatment planning for lung cancer. This is because electron transport issues, not accounted for accurately with conventional algorithms, are exacerbated in the low density tissues. A consequence of electronic disequilibrium in the lung is the underdosage of the PTV, as shown in Fig. 11. The penumbral widening in the dose distribution as a result of the increased electron scattering in the lung is illustrated for a conformal lung plan in Fig. 12. Depending on the location and size of the tumor, and the beam energy, underdosage of the PTV in lung planning may be significant. In addition to the target coverage, dose to normal tissues, particularly the normal lung, may be equally affected. Numerous lung planning studies have shown sometimes substantial differences (10%–20%) between conventional and MC algorithms.[117,190,192,214,216,242–246]

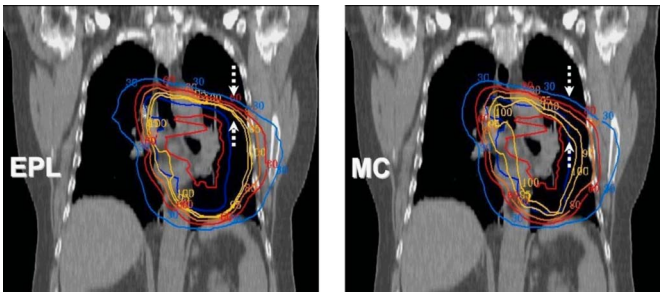

FIG. 12. Isodose distributions for a 3D conformal lung plan (15 MV photons) calculated using an equivalent path length (EPL, University of Michigan/UMPlan) algorithm on the left and a MC calculation (modified DPM, UMPlan) on the right. A distinct penumbral broadening in the MC-based dose distribution (on the right) is observed due to the increased electron scattering in the lung tissue. This effect is not as pronounced in the EPL-calculated dose distribution.

Due to the complicated dosimetric issues associated with treatment planning in the lung, more studies and comparisons using the MC method are encouraged. The utilization of advanced techniques, such as extracranial stereotactic radiotherapy using 10–24 Gy fractions,[247] for the treatment of early stage lung cancer, may increase the importance of accurate dosimetry and the clinical importance of MC calculated doses. One of the important next steps must be to evaluate how the improved MC dose distributions will clinically impact outcome for tumors and normal tissues.

IV.B.1.b. Head and neck There have been numerous studies on MC head and neck CRT and IMRT planning.[190,192,193,214,248–250] These studies have shown in general that dose differences between convolution and MC algorithms are dosimetrically insignificant. However, it has also been shown that dose differences for tumors located in the presence of air cavities can be significant due to inaccurate calculation of the photon/electron energy fluence inside and around air cavities using Batho and ETAR methods[214] as well as a collapsed cone convolution algorithm.[250,251]

IV.B.1.c. Other treatment sites Readers are encouraged to review articles published on MC-based treatment planning in other anatomical sites, which include: brain,[89,91,219,252–254] breast,[216,255] and prostate.[193,214,216,256,257]

IV.B.2. Electron beam treatment planning

There have been numerous studies on the use of MC calculations in electron beam treatment planning.[26,111,115,121,258–262] In some instances, significant differences between pencil beam dose distributions and MC calculations have been demonstrated, particularly in regions in or near air cavities and lung or bone tissues.[115,263] Large differences have also been observed for small irregular fields, beams with oblique incidence, and for extended SSD treatments.[115,263] The use of the MC method represents a significant improvement in accuracy for electron beam dose calculation compared with conventional algorithms. Electron MC calculations require far fewer primary histories to achieve a given uncertainty on the dose being calculated because electrons deposit their energy in a more continuous manner, in a smaller volume and mostly starting from the same location (the patient surface). This timing advantage has allowed the development of commercial electron beam MC algorithms which are time efficient (taking on the order of minutes per plan) even on a single processor.[26]

From phantom and routine patient planning calculations based on experience with a commercial electron beam MC algorithm (VMC++, currently Nucletron), Cygler *et al.*[26] have reported that MC-generated monitor unit (MU) values may differ from the homogeneous (water phantom) values by as much as 10%, depending on surface irregularities and inhomogeneities present in the irradiated volume. This situation is frequently encountered for head and neck sites, especially in the region of the nasal cavities. In such cases, surface irregularities and missing tissue lateral to the air cavity necessitate larger MUs to deliver the same prescribed dose versus flat surface anatomies. As is the case with photon beams,

it is important that the statistical uncertainties in the single voxel MU calculations be reported.

IV.C. Association of Monte Carlo calculated dose distributions with clinical outcome

As with other changes to the therapy treatment process, with the implementation of a new dose calculation algorithm such as the MC method, users should correlate doses and prescriptions with respect to previous clinical experience.

Chetty *et al.*[238] studied dose-effect relationships (for tumor and normal tissues) by recalculating dose distributions retrospectively using the MC method for patients treated on a nonsmall cell lung cancer (NSCLC) dose escalation protocol[264]—original plans were generated using an EPL algorithm. Follow-up data was evaluated from CT scans taken six months to two years postradiation therapy. Follow-up CT scans were fused with initial treatment planning scans and the original and replanned dose distributions were mapped onto the anatomy to establish associations between dose and regions of local recurrence and normal lung damage (radiation-induced pneumonitis).[238] Preliminary results of this study showed that the originally planned PTVs are sometimes significantly underdosed with MC calculations compared with the EPL algorithm.[238] For normal lung tissue, the correlation of dose with normal tissue complications was also found to differ, but also showed that beam model differences (not related to the dose calculation algorithm in the patient) are important and must be considered for an unbiased comparison of dose calculated by different algorithms.[136,238,241,265]

Lindsay *et al.*[239] performed retrospective MC-based recalculations of a large group of lung cancer treatment plans and showed significant differences in dose indices (V20, maximum lung dose and mean GTV dose) between plans without heterogeneity correction and MC calculations. Moreover, correlations between V20 and observed radiation pneumonitis in this study were found to be different between plans without heterogeneity correction and MC-based treatment plans.[239]

Despite the preliminary (and somewhat anecdotal) nature of the evidence thus far, observations suggest that more accurate dose calculations will reveal inadequate target coverage or hot spots in certain areas of organs at risk that could lead to differences in outcome. Complete MC recalculations of delivered dose distributions that include the effects of other factors, such as organ motion and patient setup errors, will be required to refine these correlation studies. In addition, it should be noted that the efficacy of radiation therapy is also dependent upon individual patient response.

The clinical evidence thus far, albeit preliminary and retrospective, provides support that dose delivery based on MC treatment plans, particularly for lung cancer, have the potential to result in clinically significant changes. Kong *et al.*[266] have shown that dose significantly impacts local control and overall survival for NSCLC; local control was found to increase at a rate of 1.3% per gray above the conventional dose fractionation scheme (63–69 Gy in 2.0 Gy fractions). This suggests that even small differences in dose distributions, as a result of inaccurate dose calculation, are likely to affect local control and survival for patients with NSCLC. Further studies of MC dose distributions in the lung and in other sites, such as the head/neck, are necessary and are encouraged in order to unequivocally evaluate the clinical utility of MC-calculated doses.

V. SUMMARY

We wish to reiterate that, from a clinical implementation standpoint, the MC method should be treated as would any conventional dose algorithm. Proper implementation will require the clinical physicist to understand, on some level, the fundamentals of the algorithm as well as the possible pitfalls associated with its clinical implementation, much as one would for any dose algorithm. In addition to providing an educational review of the MC dose calculation method, we have identified issues that will need to be considered by developers, vendors, and end users of MC-based techniques, ultimately to ensure that patient dose calculations are effected safely.

In conclusion, we present a summary of some of the issues which are important in the implementation and clinical use of MC dose calculation algorithms. The recommendations summarized here are not meant to be prescriptive; rather they are intended as a preliminary guide for medical physicists to ensure thoughtful and safe implementation of clinical MC algorithms. We anticipate that many of the areas of concern will be studied in further detail in future, more specific task group reports.

V.A. Treatment head simulation

(a) Vendors of MC-based dose calculation systems should be responsible for providing the necessary guidance and assistance with the beam modeling and benchmarking process. Such guidance includes the tuning of parameters such as the electron energy, or the adjustment of model parameters (in measurement-driven models) to ensure that the beam model meets the required specifications.

(b) In reporting statistical uncertainties in the calculated patient dose, vendors should properly account for latent variance in the beam model if the model is based on treatment head simulation. Further, if the latent variance is a significant contributor to the total variance the number of phase-space particles in the beam simulation should be increased.

V.B. Patient simulation

V.B.1. Statistical uncertainties

We recommend that quantities, such as $\boldsymbol{F}_{\boldsymbol{D}>0.5\boldsymbol{D}_{\max}}$, or $\boldsymbol{F}_{\mathrm{PTV}}$, or $\boldsymbol{F}_{\mathrm{PRV}}$ for doses to the specific volumes, PTV or PRV respectively, be adopted as a standard method of reporting fractional statistical uncertainties in dose averaged over the relevant volume. The sole use of dose uncertainties to indi-

vidual voxels, such as the maximum dose voxel, D_{max}, should be avoided. Additionally, reporting of single voxel doses or doses over patient subvolumes should be accompanied by their respective statistical uncertainties. In situations where doses in individual voxels are important, such as D_{max} to a serial organ like the spinal cord, it may be necessary to simulate a large enough number of histories so that $s_{D_{max}}$ is very small. This will ensure that the absolute uncertainty in D_{max} will also be small. The required statistical precision required for individual voxel dose estimates should be decided upon with guidance from the clinical team.

V.B.2. Variance reduction techniques, efficiency enhancing methods, and other parameters

Users should understand the influence on the dose accuracy of variance reduction implementations and approximate methods used to improve the calculation efficiency, as well as any other accessible parameters of importance to the MC dose algorithm. Appropriate documentation on the methods used and their influence should be made available to the user. More studies on the influence of efficiency enhancing methods in clinical treatment planning are warranted, as it is likely that the tradeoffs between speed and accuracy will not be the same in different anatomical sites.[267] Where possible, vendors should provide users with the flexibility to adjust parameter inputs for these efficiency enhancement techniques but implement default values which are conservative, i.e., accurate in all situations.

V.B.3. Dose prescriptions

Vendors are strongly discouraged from using single voxel (point) doses for dose prescription and monitor unit calculations in their MC-based treatment planning systems. Rather, doses should be prescribed to volumes larger than a single voxel, such as the volume contained by an isodose surface. Current users of MC-based planning systems are encouraged to find ways of circumventing point-based dose prescriptions if their systems are not flexible enough to allow otherwise.

V.B.4. CT-to-material conversions

The use of conversion techniques based purely on mass density (i.e., assuming the only patient material is water, but with varying density), as employed in conventional algorithms, is discouraged with MC simulation because these methods ignore dependencies of particle interactions on the materials, which can lead to notable discrepancies in high atomic number materials. The conversions should include the use of both mass density and the atomic compositions of the materials. Appropriate documentation on the CT number-to-material conversion method used by the software should be accessible to the user.

V.B.5. Dose-to-water and dose-to-medium

MC dose results should: (a) explicitly indicate the material to which the dose is computed, (b) allow conversion between D_m and D_w using the methods discussed in Sec. III D 4, or other methods as developed in future investigations. It is strongly encouraged that appropriate documentation on the dose-to-water conversion method used by the software be provided to the user.

V.C. Experimental verification

V.C.1. Examples of specific tests

In addition to the standard testing necessary for conventional dose algorithms, it is strongly recommended that additional tests (e.g., as suggested in Sec. III E 3) be included to evaluate the accuracy of MC calculations under situations where the MC method is known to perform better than conventional algorithms.

V.C.2. Verification calculations

MC verification calculations should be performed under the same conditions as the experiments. Phantoms used should be CT-imaged for planning purposes. Statistical uncertainties for verification plans should be reported and included in the comparison of calculations with measurements. More studies of the influence of detector perturbations using MC calculations are encouraged.

V.C.3. Measurement uncertainties

It is important for the user to understand the limitations of the various measurement devices as they are used in different situations. It is recommended that realistic measurement uncertainties be assessed and included when evaluating MC verification calculations against measurements.

Although the implementation of MC treatment planning will require clinical physicists to once again understand a new technology, one should view this in a positive light. Properly implemented MC algorithms will provide dose calculation with sufficient accuracy (in at least a single instance of the patient geometry) such that dose calculation is no longer a source of meaningful uncertainty in the radiotherapy planning process. In addition, although the details are sometimes complex, the underlying idea of simulating the actual transport of individual particles is simpler to understand than many other algorithms because it is based on actual physical processes familiar to the medical physicist. Finally, this may well be the last new dose calculation algorithm that medical physicists will need to learn since MC techniques provide the highest level of accuracy for dose calculations in radiotherapy treatment planning.

ACKNOWLEDGMENTS

I.J.C. acknowledges the support of his colleagues, in particular, Dick Fraass, Daniel McShan, and Randy Ten Haken, at the University of Michigan, Department of Radiation Oncology. Thanks to Neelam Tyagi and Mihaela Rosu for their help with compiling references. We are grateful to Lesley Buckley, Dan La Russa, and Randy Taylor of Carleton University for commenting on early versions of the manuscript. I.J.C. is thankful to Alex Bielajew for helpful discussions on various topics in this report. I.J.C. acknowledges the support

of NIH Grant Nos. R01CA106770 (UNMC) and P01CA59827 (previously at the University of Michigan). D.W.O.R. is supported by the Canada Research Chairs program and the Natural Sciences and Engineering Research Council of Canada. B.A.F. acknowledges the support of NIH Grant No. R01CA104777. J.V.S. acknowledges the support of NIH Grant No. R01CA98524. J. S. is a research scientist of the National Cancer Institute Canada supported with funds from the Canadian Cancer Society. Finally, we are indebted to Alan Nahum for his careful review of this report which helped us improve the pedagogical aspects and other topics significantly.

[a]Electronic mail: ichetty@unmc.edu

[1]N. Papanikolaou, J. Battista, A. Boyer, C. Kappas, E. Klein, T. Mackie, M. Sharpe, and J. Van Dyk, "AAPM Report No. 85: Tissue inhomogeneity corrections for megavoltage photon beams," in *AAPM Report No. 85* (Medical Physics, Madison, WI, 2004), pp. 1–135.

[2]A. Dutreix, "When and how can we improve precision in radiotherapy?," Radiother. Oncol. **2**, 275–292 (1984).

[3]C. G. Orton, P. M. Mondalek, J. T. Spicka, D. S. Herron, and L. I. Andres, "Lung corrections in photon beam treatment planning: Are we ready?," Int. J. Radiat. Oncol. Biol. Phys. **10**, 2191–2199 (1984).

[4]J. G. Stewart and A. W. Jackson, "The steepness of the dose response curve both for tumor cure and normal tissue injury," Laryngoscope **85**, 1107–1111 (1975).

[5]M. Goitein and J. Busse, "Immobilization error: Some theoretical considerations," Radiology **117**, 407–412 (1975).

[6]http://eom.springer.de/B/b017750.htm

[7]N. Metropolis, "The beginning of the MC Method," Los Alamos Sci. **15**, 125–130 (1987); see http://library.lanl.gov/la-pubs/00326866.pdf.

[8]D. W. O. Rogers and A. F. Bielajew, in *The Dosimetry of Ionizing Radiation*, edited by B. Bjarngard, K. Kase, and F. Attix (Academic, New York, 1990), Vol. III, pp. 427–539.

[9]M. J. Berger, in *Methods in Computational Physics*, edited by S. Fernbach, B. Alder, and M. Rothenberg (Academic, New York, 1963), Vol. 1.

[10]M. Berger and S. Seltzer, "ETRAN Monte Carlo code system for electron and photon transport through extended media," Radiation Shielding Information Center (RSIC) Report CCC-107, Oak Ridge National Laboratory, Oak Ridge, TN, 1973.

[11]J. F. Briesmeister, "MCNP—A general Monte Carlo *N* -particle transport code, version 4A," Report LA-12625-M, Los Alamos National Laboratory, Los Alamos, NM, 1993.

[12]W. R. Nelson, H. Hirayama, and D. W. O. Rogers, "The EGS4 code system," Report SLAC-265, Stanford Linear Accelerator, Stanford, CA, 1985.

[13]P. L. Petti, M. S. Goodman, T. A. Gabriel, and R. Mohan, "Investigation of buildup dose from electron contamination of clinical photon beams," Med. Phys. **10**, 18–24 (1983).

[14]R. Mohan, C. Chui, and L. Lidofsky, "Energy and angular distributions of photons from medical linear accelerators," Med. Phys. **12**, 592–597 (1985).

[15]M. Udale, "A Monte Carlo investigation of surface doses for broad electron beams," Phys. Med. Biol. **33**, 939–954 (1988).

[16]R. L. Ford and W. R. Nelson, "The EGS code system—Version 3," Report SLAC-210, Stanford Linear Accelerator, Stanford, CA, 1978.

[17]I. Kawrakow and D. W. O. Rogers, "The EGSnrc code system: Monte Carlo simulation of electron and photon transport," Technical Report PIRS-701, National Research Council of Canada, Ottawa, Ontario, 2000.

[18]P. R. Almond, P. J. Biggs, B. M. Coursey, W. F. Hanson, M. S. Huq, R. Nath, and D. W. O. Rogers, "AAPM's TG-51 protocol for clinical reference dosimetry of high-energy photon and electron beams," Med. Phys. **26**, 1847–1870 (1999).

[19]B. A. Faddegon, P. O'Brien, and D. L. Mason, "The flatness of Siemens linear accelerator x-ray fields," Med. Phys. **26**, 220–228 (1999).

[20]M. B. Tacke, H. Szymanowski, U. Oelfke, C. Schulze, S. Nuss, E. Wehrwein, and S. Leidenberger, "Assessment of a new multileaf collimator concept using GEANT4 Monte Carlo simulations," Med. Phys. **33**, 1125–1132 (2006).

[21]A. Ito, in *Monte Carlo Transport of Electrons and Photons*, edited by W. R. Nelson, T. M. Jenkins, A. Rindi, A. E. Nahum, and D. W. O. Rogers (Plenum, New York, 1988), pp. 573–598.

[22]A. E. Nahum, in *Monte Carlo Transport of Electrons and Photons*, edited by W. R. Nelson, T. M. Jenkins, A. Rindi, A. E. Nahum, and D. W. O. Rogers (Plenum, New York, 1988), pp. 3–20.

[23]D. W. O. Rogers, B. A. Faddegon, G. X. Ding, C. M. Ma, J. We, and T. R. Mackie, "BEAM: A Monte Carlo code to simulate radiotherapy treatment units," Med. Phys. **22**, 503–524 (1995).

[24]C.-M. Ma and S. B. Jiang, "Monte Carlo modelling of electron beams from medical accelerators," Phys. Med. Biol. **44**, R157–R189 (1999).

[25]F. Verhaegen and J. Seuntjens, "Monte Carlo modelling of external radiotherapy photon beams," Phys. Med. Biol. **48**, R107–R164 (2003).

[26]J. E. Cygler, G. M. Daskalov, G. H. Chan, and G. X. Ding, "Evaluation of the first commercial Monte Carlo dose calculation engine for electron beam treatment planning," Med. Phys. **31**, 142–153 (2004).

[27]C. L. Hartmann Siantar, "Description and dosimetric verification of the PEREGRINE Monte Carlo dose calculation system for photon beams incident on a water phantom," Med. Phys. **28**, 1322–1337 (2001).

[28]P. Andreo, "Monte Carlo techniques in medical radiation physics," Phys. Med. Biol. **36**, 861–920 (1991).

[29]D. E. Raeside, "Monte Carlo principles and applications," Phys. Med. Biol. **21**, 181–197 (1976).

[30]D. W. O. Rogers, "Fifty years of Monte Carlo simulations for medical physics," Phys. Med. Biol. **51**, R287–R301 (2006).

[31]J. E. Turner, H. A. Wright, and R. N. Hamm, "A Monte Carlo primer for health physicists," Health Phys. **48**, 717–733 (1985).

[32]F. B. Brown, "MCNP—A general Monte Carlo-particle transport code, version 5," Report LA-UR-03 1987, Los Alamos National Laboratory, Los Alamos, NM, 2003.

[33]S. Agostinelli, "GEANT4—A simulation toolkit," Nucl. Instrum. Methods Phys. Res. A **506**, 250–303 (2003).

[34]J. Baro, J. Sempau, J. M. Fernandez-Varea, and F. Salvat, "PENELOPE—An algorithm for Monte-Carlo simulation of the penetration and energy-loss of electrons and positrons in matter," Nucl. Instrum. Methods Phys. Res. A **100**, 31–46 (1995).

[35]M. Fippel, "Fast Monte Carlo dose calculation for photon beams based on the VMC electron algorithm," Med. Phys. **26**, 1466–1475 (1999).

[36]I. Kawrakow, "VMC++ , electron and photon Monte Carlo calculations optimized for radiation treatment planning," in *Advanced Monte Carlo for Radiation Physics, Particle Transport Simulation and Applications: Proceedings of the Monte Carlo 2000 Meeting Lisbon*, edited by A. Kling, F. Barao, M. Nakagawa, L. Tavora, and P. Vaz (Springer, Berlin, 2001), pp. 229–236.

[37]I. Kawrakow, M. Fippel, and K. Friedrich, "3D electron dose calculation using a Voxel based Monte Carlo algorithm (VMC)," Med. Phys. **23**, 445–457 (1996).

[38]H. Neuenschwander and E. J. Born, "A macro Monte-Carlo method for electron-beam dose calculations," Phys. Med. Biol. **37**, 107–125 (1992).

[39]J. Sempau, S. J. Wilderman, and A. F. Bielajew, "DPM, a fast, accurate Monte Carlo code optimized for photon and electron radiotherapy treatment planning dose calculations," Phys. Med. Biol. **45**, 2263–2291 (2000).

[40]I. Kawrakow, "Accurate condensed history Monte Carlo simulation of electron transport. I. EGSnrc, the new EGS4 version," Med. Phys. **27**, 485–498 (2000).

[41]A. F. Bielajew and D. W. O. Rogers, in *Monte Carlo Transport of Electrons and Photons*, edited by W. R. Nelson, T. M. Jenkins, A. Rindi, A. E. Nahum, and D. W. O. Rogers (Plenum, New York, 1988), pp. 115–137.

[42]I. Kawrakow and A. F. Bielajew, "On the condensed history technique for electron transport," Nucl. Instrum. Methods Phys. Res. B **142**, 253–280 (1998).

[43]E. W. Larsen, "A theoretical derivation of the condensed history algorithm," Ann. Nucl. Energy **19**, 701–714 (1992).

[44]I. Kawrakow, "Accurate condensed history Monte Carlo simulation of electron transport. II. Application to ion chamber response simulations," Med. Phys. **27**, 499–513 (2000).

[45]I. Kawrakow and M. Fippel, "Investigation of variance reduction techniques for Monte Carlo photon dose calculation using XVMC," Phys. Med. Biol. **45**, 2163–2183 (2000).

[46]I. Kawrakow, D. W. O. Rogers, and B. R. B. Walters, "Large efficiency improvements in BEAMnrc using directional bremsstrahlung splitting," Med. Phys. **31**, 2883–2898 (2004).

[47]I. Kawrakow and B. R. B. Walters, "Efficient photon beam dose calculations using DOSXYZnrc with BEAMnrc," Med. Phys. **33**, 3046–3056 (2006).
[48]B. Fraass, K. Doppke, M. Hunt, G. Kutcher, G. Starkschall, R. Stern, and J. Van Dyke, "American Association of Physicists in Medicine Radiation Therapy Committee Task Group 53: Quality assurance for clinical radiotherapy treatment planning," Med. Phys. **25**, 1773–1829 (1998).
[49]IAEA-Technical Report Series No. 430: Commissioning and quality qs-surance of computerized planning systems for radiation treatment of cancer," in International Atomic Energy Agency, Vienna, 2004.
[50]J. Van Dyk, R. B. Barnett, J. E. Cygler, and P. C. Shragge, "Commissioning and quality assurance of treatment planning computers," Int. J. Radiat. Oncol. Biol. Phys. **26**, 261–273 (1993).
[51]D. W. O. Rogers and A. F. Bielajew, in *Monte Carlo Transport of Electrons and Photons*, edited by W. R. Nelson, T. M. Jenkins, A. Rindi, A. E. Nahum, and D. W. O. Rogers (Plenum, New York, 1988), pp. 407–419.
[52]I. Kawrakow, "On the efficiency of photon beam treatment head simulations," Med. Phys. **32**, 2320–2326 (2005).
[53]C.-M. Ma *et al.*, "A Monte Carlo dose calculation tool for radiotherapy treatment planning," Phys. Med. Biol. **47**, 1671–1689 (2002).
[54]J. A. Halbleib, in *Monte Carlo Transport of Electrons and Photons*, edited by W. R. Nelson, T. M. Jenkins, A. Rindi, A. E. Nahum, and D. W. O. Rogers (Plenum, New York, 1988), pp. 249–262.
[55]J. A. Halbleib and T. A. Melhorn, "ITS: The integrated TIGER series of coupled electron/photon Monte Carlo transport codes," Sandia Report SAND84–0573, Sandia National Laboratory, Albuquerque, NM, 1984.
[56]S. M. Seltzer, in *Monte Carlo Transport of Electrons and Photons*, edited by W. R. Nelson, T. M. Jenkins, A. Rindi, A. E. Nahum, and D. W. O. Rogers (Plenum, New York, 1988), pp. 153–182.
[57]D. W. O. Rogers, B. Walters, and I. Kawrakow, "BEAMnrc Users Manual," NRC Report PIRS 509(a)revH, 2004.
[58]B. R. B. Walters and D. W. O. Rogers, "DOSXYZnrc Users Manual," NRC Report PIRS 794 (rev B), 2004.
[59]D. W. O. Rogers, "The role of Monte-Carlo simulation of electron-transport in radiation-dosimetry," Appl. Radiat. Isot. **42**, 965–974 (1991).
[60]T. R. Mackie, S. S. Kubsad, D. W. O. Rogers, and A. F. Bielajew, "The OMEGA project: Electron dose planning using Monte Carlo simulation," Med. Phys. **17**, 730 (abstract) (1990).
[61]J. Siebers and R. Mohan, "Monte Carlo and IMRT," in *Intensity Modulated Radiation Therapy, The State of the Art, Proceedings of the 2003 AAPM Summer School*, edited by T. R. Mackie and J. R. Palta (Advanced Medical, Madison, WI, 2003), pp. 531–560.
[62]A. Leal, F. Sanchez-Doblado, R. Arrans, M. Perucha, M. Rincon, E. Carrasco, and C. Bernal, "Monte Carlo simulation of complex radiotherapy treatments," Comput. Sci. Eng. **6**, 60–68 (2004).
[63]N. Tyagi, A. Bose, and I. J. Chetty, "Implementation of the DPM Monte Carlo Code on a parallel architecture for treatment planning applications," Med. Phys. **31**, 2721–2725 (2004).
[64]J. M. Fernandez-Varea, R. Mayol, J. Baro, and F. Salvat, "On the theory and simulation of multiple elastic-scattering of electrons," Nucl. Instrum. Methods Phys. Res. B **73**, 447–473 (1993).
[65]A. E. Schach von Wittenau, L. J. Cox, P. M. Bergstrom, Jr., W. P. Chandler, C. L. Hartmann Siantar, and R. Mohan, "Correlated histogram representation of Monte Carlo derived medical accelerator photon-output phase space," Med. Phys. **26**, 1196–1211 (1999).
[66]A. E. Schach von Wittenau, P. M. Bergstrom, Jr., and L. J. Cox, "Patient-dependent beam-modifier physics in Monte Carlo photon dose calculations," Med. Phys. **27**, 935–947 (2000).
[67]I. Kawrakow, "Electron transport: Multiple and plural scattering," Nucl. Instrum. Methods Phys. Res. B **108**, 23–34 (1996).
[68]I. Kawrakow and A. F. Bielajew, "Recent improvements and accuracy tests of the VOXEL Monte Carlo algorithm," Med. Phys. **24**, 1049 (abstract) (1997).
[69]P. J. Keall and P. W. Hoban, "Superposition dose calculation incorporating Monte Carlo generated electron track kernels," Med. Phys. **23**, 479–485 (1996).
[70]L. Wang, C. S. Chui, and M. Lovelock, "A patient-specific Monte Carlo dose-calculation method for photon beams," Med. Phys. **25**, 867–878 (1998).
[71]R. Doucet, M. Olivares, F. DeBlois, E. B. Podgorsak, I. Kawrakow, and J. Seuntjens, "Comparison of measured and Monte Carlo calculated dose distributions in inhomogeneous phantoms in clinical electron beams," Phys. Med. Biol. **48**, 2339–2354 (2003).
[72]M. Fippel, "Efficient particle transport simulation through beam modulating devices for Monte Carlo treatment planning," Med. Phys. **31**, 1235–1242 (2004).
[73]M. Fippel, F. Haryanto, O. Dohm, F. Nusslin, and S. Kriesen, "A virtual photon energy fluence model for Monte Carlo dose calculation," Med. Phys. **30**, 301–311 (2003).
[74]M. Fippel, I. Kawrakow, and K. Friedrich, "Electron beam dose calculations with the VMC algorithm and the verification data of the NCI working group," Phys. Med. Biol. **42**, 501–520 (1997).
[75]M. Fippel, W. Laub, B. Huber, and F. Nusslin, "Experimental investigation of a fast Monte Carlo photon beam dose calculation algorithm," Phys. Med. Biol. **44**, 3039–3054 (1999).
[76]M. Fippel and F. Nusslin, "Evaluation of a clinical Monte Carlo dose calculation code based on the ICCR benchmark test," Med. Phys. **28**, 1198 (abstract) (2001).
[77]I. Kawrakow and A. F. Bielajew, "On the representation of electron multiple elastic-scattering distributions for Monte Carlo calculations," Nucl. Instrum. Methods Phys. Res. B **134**, 325–336 (1998).
[78]H. Neuenschwander, T. R. Mackie, and P. J. Reckwerdt, "MMC—A high-performance Monte Carlo code for electron beam treatment planning," Phys. Med. Biol. **40**, 543–574 (1995).
[79]C. Cris, E. Born, R. Mini, H. Neuenschwander, and W. Volken, "A scaling method for multiple source models," in *Proceedings of the 13th ICCR*, edited by T. Bortfeld and W. Schlegel (Springer-Verlag, Heidelberg, 2000), pp. 411–413.
[80]P. Pemler, J. Besserer, U. Schneider, and H. Neuenschwander, "Evaluation of a commercial electron treatment planning system based on Monte Carlo techniques (eMC)," Z. Med. Phys. **16**, 313–329 (2006).
[81]C.-M. Ma, J. S. Li, T. Pawlicki, S. B. Jiang, and J. Deng, "MCDOSE—A Monte Carlo dose calculation tool for radiation therapy treatment planning," in *Proceedings of the 13th ICCR*, edited by T. Bortfeld and W. Schlegel (Springer-Verlag, Heidelberg, 2000), pp. 411–413.
[82]J. V. Siebers, P. J. Keall, J. Kim, and R. Mohan, "Performance benchmarks of the MCV Monte Carlo System," in *Proceedings of the 13th ICCR*, edited by T. Bortfeld and W. Schlegel (Springer-Verlag, Heidelberg, 2000), pp. 129–131.
[83]J. V. Siebers, P. J. Keall, J. O. Kim, and R. Mohan, "A method for photon beam Monte Carlo multileaf collimator particle transport," Phys. Med. Biol. **47**, 3225–3249 (2002).
[84]I. J. Chetty, P. M. Charland, N. Tyagi, D. L. McShan, B. A. Fraass, and A. F. Bielajew, "Photon beam relative dose validation of the DPM Monte Carlo code in lung-equivalent media," Med. Phys. **30**, 563–573 (2003).
[85]I. J. Chetty, N. Tyagi, M. Rosu, P. M. Charland, D. L. McShan, R. K. Ten Haken, B. A. Fraass, and A. F. Bielajew, "Clinical implementation, validation and use of the DPM Monte Carlo code for radiotherapy treatment planning," in *Nuclear Mathematical and Computational Sciences: A Century in Review, A Century Anew, Gatlinburg, TN* (American Nuclear Society, LaGrange Park, IL, 2003), Vol. 119, pp. 1–17.
[86]J. J. DeMarco, T. D. Solberg, and J. B. Smathers, "A CT-based Monte Carlo simulation tool for dosimetry planning and analysis," Med. Phys. **25**, 1–11 (1998).
[87]R. F. Aaronson, J. J. DeMarco, I. J. Chetty, and T. D. Solberg, "A Monte Carlo based phase space model for quality assurance of intensity modulated radiotherapy incorporating leaf specific characteristics," Med. Phys. **29**, 2952–2958 (2002).
[88]I. Chetty, J. J. DeMarco, and T. D. Solberg, "A virtual source model for Monte Carlo modeling of arbitrary intensity distributions," Med. Phys. **27**, 166–172 (2000).
[89]I. J. Chetty, J. J. DeMarco, T. D. Solberg, A. R. Arellano, R. Fogg, and A. V. Mesa, "A phase space model for simulating arbitrary intensity distributions for shaped radiosurgery beams using the Monte Carlo method," Radiosurgery **3**, 41–52 (2000).
[90]T. D. Solberg *et al.*, "A review of radiation dosimetry applications using the MCNP Monte Carlo code," Radiochim. Acta **89**, 337–355 (2001).
[91]T. D. Solberg, J. J. DeMarco, F. E. Holly, J. B. Smathers, and A. A. F. DeSalles, "Monte Carlo treatment planning for stereotactic radiosurgery," Radiother. Oncol. **49**, 73–84 (1998).
[92]M. K. Fix, P. Manser, E. J. Born, R. Mini, and P. Ruegsegger, "Monte Carlo simulation of a dynamic MLC based on a multiple source model," Phys. Med. Biol. **46**, 3241–3257 (2001).
[93]M. K. Fix, M. Stampanoni, P. Manser, E. J. Born, R. Mini, and P. Ruegsegger, "A multiple source model for 6 MV photon beam dose calculations using Monte Carlo," Phys. Med. Biol. **46**, 1407–1427 (2001).

[94]E. Poon and F. Verhaegen, "Accuracy of the photon and electron physics in GEANT4 for radiotherapy applications," Med. Phys. **32**, 1696–1711 (2005).
[95]J. Sempau, A. Sanchez-Reyes, and F. Salvat, "H. O. ben Tahar, S. B. Jiang, and J. M. Fernandez-Varea, "Monte Carlo simulation of electron beams from an accelerator head using PENELOPE," Phys. Med. Biol. **46**, 1163–1186 (2001).
[96]O. Chibani and X. A. Li, "Monte Carlo dose calculations in homogeneous media and at interfaces: A comparison between GEPTS, EGSnrc, MCNP, and measurements," Med. Phys. **29**, 835–847 (2002).
[97]O. Chibani and C. M. Ma, "Electron depth dose distributions in water, iron and lead: The GEPTS system," Nucl. Instrum. Methods Phys. Res. B **101**, 357–378 (1995).
[98]W. van der Zee, A. Hogenbirk, and S. C. van der Marck, "ORANGE: A Monte Carlo dose engine for radiotherapy," Phys. Med. Biol. **50**, 625–641 (2005).
[99]D. W. O. Rogers and R. Mohan, "Questions for comparisons of clinical Monte Carlo codes," in *Proceedings of the 13th ICCR*, edited by T. Bortfeld and W. Schlegel (Springer-Verlag, Heidelberg, 2000), pp. 120–122.
[100]B. A. Faddegon and I. Blevis, "Electron spectra derived from depth dose distributions," Med. Phys. **27**, 514–526 (2000).
[101]M. R. Bieda, J. A. Antolak, and K. R. Hogstrom, "The effect of scattering foil parameters on electron-beam Monte Carlo calculations," Med. Phys. **28**, 2527–2534 (2001).
[102]D. Sheikh-Bagheri and D. W. O. Rogers, "Sensitivity of megavoltage photon beam Monte Carlo simulations to electron beam and other parameters," Med. Phys. **29**, 379–390 (2002).
[103]A. Tzedakis, J. E. Damilakis, M. Mazonakis, J. Stratakis, H. Varveris, and N. Gourtsoyiannis, "Influence of initial electron beam parameters on Monte Carlo calculated absorbed dose distributions for radiotherapy photon beams," Med. Phys. **31**, 907–913 (2004).
[104]I. J. Chetty, P. M. Charland, N. Tyagi, D. L. McShan, B. Fraass, and A. F. Bielajew, "Experimental validation of the DPM Monte Carlo code for photon beam dose calculations in inhomogeneous media," Med. Phys. **29**, 1351 (abstract) (2002).
[105]B. Libby, J. Siebers, and R. Mohan, "Validation of Monte Carlo generated phase-space descriptions of medical linear accelerators," Med. Phys. **26**, 1476–1483 (1999).
[106]C. Bramoulle, F. Husson, and J. P. Manens, "Monte Carlo (PENELOPE code) study of the x-ray beams from SL Linacs (Elekta)," Phys. Med. **16**, 107–115 (2000).
[107]E. L. Chaney, T. J. Cullip, and T. A. Gabriel, "A Monte Carlo study of accelerator head scatter," Med. Phys. **21**, 1383–1390 (1994).
[108]G. X. Ding, "Energy spectra, angular spread, fluence profiles and dose distributions of 6 and 18 MV photon beams: Results of Monte Carlo simulations for a Varian 2100EX accelerator," Phys. Med. Biol. **47**, 1025–1046 (2002).
[109]R. A. C. Siochi, "Requirements for manufacturer supplied data for Monte Carlo simulation," in *Proceedings of the 15th International Conference on the Applications of Accelerators in Research and Industry* (The American Institute of Physics, Melville, 1999), pp. 1060–1065.
[110]G. G. Zhang, D. W. O. Rogers, J. E. Cygler, and T. R. Mackie, "Monte Carlo investigation of electron beam output factors versus size of square cutout," Med. Phys. **26**, 743–750 (1999).
[111]J. A. Antolak, M. R. Bieda, and K. R. Hogstrom, "Using Monte Carlo methods to commission electron beams: A feasibility study," Med. Phys. **29**, 771–786 (2002).
[112]B. Faddegon, E. Schreiber, and X. Ding, "Monte Carlo simulation of large electron fields," Phys. Med. Biol. **50**, 741–753 (2005).
[113]E. C. Schreiber and B. A. Faddegon, "Sensitivity of large-field electron beams to variations in a Monte Carlo accelerator model," Phys. Med. Biol. **50**, 769–778 (2005).
[114]C.-M. Ma, B. A. Faddegon, D. W. O. Rogers, and T. R. Mackie, "Accurate characterization of Monte Carlo calculated electron beams for radiotherapy," Med. Phys. **24**, 401–416 (1997).
[115]C.-M. Ma, E. Mok, A. Kapur, T. Pawlicki, D. Findley, S. Brain, K. Forster, and A. L. Boyer, "Clinical implementation of a Monte Carlo treatment planning system," Med. Phys. **26**, 2133–2143 (1999).
[116]C.-M. Ma and D. W. O. Rogers, "BEAM Characterization: A Multiple-Source Model," NRC Report PIRS-0509(C), 1995.
[117]C.-M. Ma, "Characterization of computer simulated radiotherapy beams for Monte-Carlo treatment planning," Radiat. Phys. Chem. **53**, 329–344 (1998).
[118]J. Deng, S. B. Jiang, A. Kapur, J. Li, T. Pawlicki, and C. M. Ma, "Photon beam characterization and modelling for Monte Carlo treatment planning," Phys. Med. Biol. **45**, 411–427 (2000).
[119]B. Faddegon, J. Balogh, R. Mackenzie, and D. Scora, "Clinical considerations of Monte Carlo for electron radiotherapy treatment planning," Radiat. Phys. Chem. **53**, 217–227 (1998).
[120]M. K. Fix, H. Keller, P. Ruegsegger, and E. J. Born, "Simple beam models for Monte Carlo photon beam dose calculations in radiotherapy," Med. Phys. **27**, 2739–2747 (2000).
[121]S. B. Jiang, A. Kapur, and C. M. Ma, "Electron beam modeling and commissioning for Monte Carlo treatment planning," Med. Phys. **27**, 180–191 (2000).
[122]S. B. Jiang, J. Deng, J. Li, P. Pawlicki, A. Boyer, and C.-M. Ma, "Modeling and commissioning of clinical photon beams for Monte Carlo treatment planning," in *Proceedings of the 13th ICCR*, edited by T. Bortfeld and W. Schlegel (Springer-Verlag, Heidelberg, 2000), pp. 434–436.
[123]J. Deng, S. B. Jiang, P. Pawlicki, J. Li, and C.-M. Ma, "Electron beam commissioning for Monte Carlo dose calculation," in *Proceedings of the 13th ICCR*, edited by T. Bortfeld and W. Schlegel (Springer-Verlag, Heidelberg, 2000), pp. 431–433.
[124]J. S. Li *et al.*, "Source modeling and beam commissioning for Siemens photon beams," Med. Phys. **29**, 1230 (abstract) (2002).
[125]J. Yang, J. S. Li, L. Qin, W. Xiong, and C. M. Ma, "Modelling of electron contamination in clinical photon beams for Monte Carlo dose calculation," Phys. Med. Biol. **49**, 2657–2673 (2004).
[126]J. Deng, T. Guerrero, C. M. Ma, and R. Nath, "Modelling 6 MV photon beams of a stereotactic radiosurgery system for Monte Carlo treatment planning," Phys. Med. Biol. **49**, 1689–1704 (2004).
[127]J. Deng, S. B. Jiang, T. Pawlicki, J. Li, and C. M. Ma, "Derivation of electron and photon energy spectra from electron beam central axis depth dose curves," Phys. Med. Biol. **46**, 1429–1449 (2001).
[128]J. J. Janssen, E. W. Korevaar, L. J. van Battum, P. R. Storchi, and H. Huizenga, "A model to determine the initial phase space of a clinical electron beam from measured beam data," Phys. Med. Biol. **46**, 269–286 (2001).
[129]S. Siljamaki, L. Tillikainen, H. Helminen, and J. Pyyry, "Determining parameters for a multiple-source model of a linear accelerator using optimization techniques," Med. Phys. **32**, 2113 (abstract) (2005).
[130]W. Ulmer, J. Pyyry, and W. Kaissl, "A 3D photon superposition/convolution algorithm and its foundation on results of Monte Carlo calculations," Phys. Med. Biol. **50**, 1767–1790 (2005).
[131]K. Aljarrah, G. C. Sharp, T. Neicu, and S. B. Jiang, "Determination of the initial beam parameters in Monte Carlo linac simulation," Med. Phys. **33**, 850–858 (2006).
[132]A. Ahnesjo and P. Andreo, "Determination of effective bremsstrahlung spectra and electron contamination for photon dose calculations," Phys. Med. Biol. **34**, 1451–1464 (1989).
[133]A. Ahnesjo and A. Trepp, "Acquisition of the effective lateral energy fluence distribution for photon beam dose calculations by convolution models," Phys. Med. Biol. **36**, 973–985 (1991).
[134]A. Ahnesjo, L. Weber, A. Murman, M. Saxner, I. Thorslund, and E. Traneus, "Beam modeling and verification of a photon beam multisource model," Med. Phys. **32**, 1722–1737 (2005).
[135]A. Catala, P. Francois, J. Bonnet, and C. Scouarnec, "Reconstruction of 12 MV bremsstrahlung spectra from measured transmission data by direct resolution of the numeric system $AF=T$," Med. Phys. **22**, 3–10 (1995).
[136]P. M. Charland, I. J. Chetty, L. D. Paniak, B. P. Bednarz, and B. A. Fraass, "Enhanced spectral discrimination through the exploitation of interface effects in photon dose data," Med. Phys. **31**, 264–276 (2004).
[137]E. Heath and J. Seuntjens, "Development and validation of a BEAMnrc component module for accurate Monte Carlo modelling of the Varian dynamic millennium multileaf collimator," Phys. Med. Biol. **48**, 4045–4063 (2003).
[138]H. H. Liu, F. Verhaegen, and L. Dong, "A method of simulating dynamic multileaf collimators using Monte Carlo techniques for intensity-modulated radiation therapy," Phys. Med. Biol. **46**, 2283–2298 (2001).
[139]N. Tyagi, J. M. Moran, D. W. Litzenberg, A. F. Bielajew, B. A. Fraass, and I. J. Chetty, "Experimental verification of a Monte Carlo-based MLC simulation model for IMRT dose calculation," Med. Phys. **34**, 651–663 (2007).
[140]T. C. Zhu *et al.*, "Output ratios in air: Report of the AAPM Task Group No. 74," Med. Phys. (submitted).
[141]T. C. Zhu and B. E. Bjarngard, "Head scatter off-axis for megavoltage x

rays," Med. Phys. **30**, 533–543 (2003).
[142]H. H. Liu, T. R. Mackie, and E. C. McCullough, "A dual source photon beam model used in convolution/superposition dose calculations for clinical megavoltage x-ray beams," Med. Phys. **24**, 1960–1974 (1997).
[143]M. B. Sharpe, D. A. Jaffray, J. J. Battista, and P. Munro, "Extrafocal radiation: A unified approach to the prediction of beam penumbra and output factors for megavoltage x-ray beams," Med. Phys. **22**, 2065–2074 (1995).
[144]H. H. Liu, T. R. Mackie, and E. C. McCullough, "Calculating output factors for photon beam radiotherapy using a convolution/superposition method based on a dual source photon beam model," Med. Phys. **24**, 1975–1985 (1997).
[145]M. R. Arnfield, J. V. Siebers, J. O. Kim, Q. Wu, P. J. Keall, and R. Mohan, "A method for determining multileaf collimator transmission and scatter for dynamic intensity modulated radiotherapy," Med. Phys. **27**, 2231–2241 (2000).
[146]H. H. Liu, T. R. Mackie, and E. C. McCullough, "Modeling photon output caused by backscattered radiation into the monitor chamber from collimator jaws using a Monte Carlo technique," Med. Phys. **27**, 737–744 (2000).
[147]S. B. Jiang, A. L. Boyer, and C. M. Ma, "Modeling the extrafocal radiation and monitor chamber backscatter for photon beam dose calculation," Med. Phys. **28**, 55–66 (2001).
[148]G. X. Ding, "Using Monte Carlo simulations to commission photon beam output factors—A feasibility study," Phys. Med. Biol. **48**, 3865–3874 (2003).
[149]B. Parker, A. S. Shiu, and H. H. Liu, "Small-field dosimetry with multiple detectors and Monte Carlo calculations," Med. Phys. **29**, 1372 (abstract) (2002).
[150]G. X. Ding, "Dose discrepancies between Monte Carlo calculations and measurements in the buildup region for a high-energy photon beam," Med. Phys. **29**, 2459–2463 (2002).
[151]G. X. Ding, C. Duzenli, and N. I. Kalach, "Are neutrons responsible for the dose discrepancies between Monte Carlo calculations and measurements in the build-up region for a high-energy photon beam?" Phys. Med. Biol. **47**, 3251–3261 (2002).
[152]W. Abdel-Rahman, J. P. Seuntjens, F. Verhaegen, F. Deblois, and E. B. Podgorsak, "Validation of Monte Carlo calculated surface doses for megavoltage photon beams," Med. Phys. **32**, 286–298 (2005).
[153]I. Kawrakow, "Efficient photon beam treatment head simulations," Radiother. Oncol. **81**, 82 (abstract) (2006).
[154]D. Sheikh-Bagheri, D. W. O. Rogers, C. K. Ross, and J. P. Seuntjens, "Comparison of measured and Monte Carlo calculated dose distributions from the NRC linac," Med. Phys. **27**, 2256–2266 (2000).
[155]I. Kawrakow, "On the effective point of measurement in megavoltage photon beams," Med. Phys. **33**, 1829–1839 (2006).
[156]O. Chibani and C. M. Ma, "On the discrepancies between Monte Carlo dose calculations and measurements for the 18 MV varian photon beam," Med. Phys. **34**, 1206–1216 (2007).
[157]W. Feller, *An Introduction to Probability Theory and Its Applications*, 3rd ed. (Wiley, New York, 1967), Vol. I.
[158]B. R. B. Walters, I. Kawrakow, and D. W. O. Rogers, "History by history statistical estimators in the BEAM code system," Med. Phys. **29**, 2745–2752 (2002).
[159]J. Sempau and A. F. Bielajew, "Towards the elimination of Monte Carlo statistical fluctuation from dose volume histograms for radiotherapy treatment planning," Phys. Med. Biol. **45**, 131–157 (2000).
[160]P. J. Keall, J. V. Siebers, R. Jeraj, and R. Mohan, "The effect of dose calculation uncertainty on the evaluation of radiotherapy plans," Med. Phys. **27**, 478–484 (2000).
[161]I. Kawrakow, "The effect of Monte Carlo statistical uncertainties on the evaluation of dose distributions in radiation treatment planning," Phys. Med. Biol. **49**, 1549–1556 (2004).
[162]I. J. Chetty, M. Rosu, M. L. Kessler, B. A. Fraass, R. K. Ten Haken, F. M. Kong, and D. L. McShan, "Reporting and analyzing statistical uncertainties in Monte Carlo-based treatment planning," Int. J. Radiat. Oncol. Biol. Phys. **65**, 1249–1259 (2006).
[163]J. V. Siebers, P. J. Keall, and I. Kawrakow, in *The Modern Technology of Radiation Oncology*, edited by J. Van Dyke (Medical Physics, Madison, WI, 2005), Vol. 2, pp. 91–130.
[164]F. M. Buffa and A. E. Nahum, "Monte Carlo dose calculations and radiobiological modelling: Analysis of the effect of the statistical noise of the dose distribution on the probability of tumour control," Phys. Med. Biol. **45**, 3009–3023 (2000).
[165]S. B. Jiang, T. Pawlicki, and C. M. Ma, "Removing the effect of statistical uncertainty on dose-volume histograms from Monte Carlo dose calculations," Phys. Med. Biol. **45**, 2151–2161 (2000).
[166]J. O. Deasy, "Denoising of electron beam Monte Carlo dose distributions using digital filtering techniques," Phys. Med. Biol. **45**, 1765–1779 (2000).
[167]I. Kawrakow, "On the de-noising of Monte Carlo calculated dose distributions," Phys. Med. Biol. **47**, 3087–3103 (2002).
[168]J. O. Deasy, M. V. Wickerhauser, and M. Picard, "Accelerating Monte Carlo simulations of radiation therapy dose distributions using wavelet threshold de-noising," Med. Phys. **29**, 2366–2373 (2002).
[169]S. J. Pollack and A. F. Bielajew, "Novel algorithms for smoothing global Monte Carlo noise," in Proceedings of the Current Topics in Monte Carlo Treatment Planning: Advanced Workshop, Montreal, CN, edited by F. Verhaegen and J. Seuntjens, 2004 (unpublished).
[170]B. Miao, R. Jeraj, S. Bao, and T. R. Mackie, "Adaptive anisotropic diffusion filtering of Monte Carlo dose distributions," Phys. Med. Biol. **48**, 2767–2781 (2003).
[171]M. Fippel and F. Nusslin, "Smoothing Monte Carlo calculated dose distributions by iterative reduction of noise," Phys. Med. Biol. **48**, 1289–1304 (2003).
[172]I. El Naqa *et al.*, "A comparison of Monte Carlo dose calculation denoising techniques," Phys. Med. Biol. **50**, 909–922 (2005).
[173]C. M. Ma, R. A. Price, Jr., J. S. Li, L. Chen, L. Wang, E. Fourkal, L. Qin, and J. Yang, "Monitor unit calculation for Monte Carlo treatment planning," Phys. Med. Biol. **49**, 1671–1687 (2004).
[174]F. C. du Plessis, C. A. Willemse, M. G. Lotter, and L. Goedhals, "The indirect use of CT numbers to establish material properties needed for Monte Carlo calculation of dose distributions in patients," Med. Phys. **25**, 1195–1201 (1998).
[175]C.-M. Ma and D. W. O. Rogers, "BEAMDP Users Manual," NRC Report PIRS-0509(D), 1995.
[176]J. V. Siebers, P. J. Keall, A. E. Nahum, and R. Mohan, "Converting absorbed dose to medium to absorbed dose to water for Monte Carlo based photon beam dose calculations," Phys. Med. Biol. **45**, 983–995 (2000).
[177]ICRU-Report No. 46: Photon, electron, proton and neutron interaction data for body tissues," in International Commission on Radiation Units and Measurements, 1992.
[178]F. Verhaegen and S. Devic, "Sensitivity study for CT image use in Monte Carlo treatment planning," Phys. Med. Biol. **50**, 937–946 (2005).
[179]M. Bazalova, L. Beaulieu, S. Palefsky, and F. Verhaegen, "Correction of CT artifacts and its influence on Monte Carlo dose calculations," Med. Phys. **34**, 2119–2132 (2007).
[180]C. Reft *et al.*, "Dosimetric considerations for patients with HIP prostheses undergoing pelvic irradiation. Report of the AAPM Radiation Therapy Committee Task Group 63," Med. Phys. **30**, 1162–1182 (2003).
[181]N. Dogan, J. V. Siebers, and P. J. Keall, "Clinical comparison of head and neck and prostate IMRT plans using absorbed dose to medium and absorbed dose to water," Phys. Med. Biol. **51**, 4967–4980 (2006).
[182]H. H. Liu, "D_m rather than D_w should be used in Monte Carlo treatment planning. For the proposition," Med. Phys. **29**, 922–923 (2002).
[183]M. Goitein, "The cell's-eye view: assessing dose in four dimensions," Int. J. Radiat. Oncol. Biol. Phys. **62**, 951–953 (2005).
[184]M. Fippel and F. Nusslin, "Comments on 'Converting absorbed dose to medium to absorbed dose to water for Monte Carlo based photon beam dose calculations'," Phys. Med. Biol. **45**, L17–L19 (2000).
[185]J. Siebers, B. Libby, and R. Mohan, "Trust, but verify: Comparison of MCNP and BEAM Monte Carlo codes for generation of phase space distributions for a Varian 2100C," Med. Phys. **25**, A143 (abstract) (1998).
[186]R. Mohan, M. Arnfield, S. Tong, Q. Wu, and J. Siebers, "The impact of fluctuations in intensity patterns on the number of monitor units and the quality and accuracy of intensity modulated radiotherapy," Med. Phys. **27**, 1226–1237 (2000).
[187]J. O. Kim, J. V. Siebers, P. J. Keall, M. R. Arnfield, and R. Mohan, "A Monte Carlo study of radiation transport through multileaf collimators," Med. Phys. **28**, 2497–2506 (2001).
[188]P. J. Keall, J. V. Siebers, M. Arnfield, J. O. Kim, and R. Mohan, "Monte Carlo dose calculations for dynamic IMRT treatments," Phys. Med. Biol. **46**, 929–941 (2001).
[189]J. V. Siebers, M. Lauterbach, P. J. Keall, and R. Mohan, "Incorporating multi-leaf collimator leaf sequencing into iterative IMRT optimization,"

Med. Phys. **29**, 952–959 (2002).
[190]L. Wang, E. Yorke, and C. S. Chui, "Monte Carlo evaluation of 6 MV intensity modulated radiotherapy plans for head and neck and lung treatments," Med. Phys. **29**, 2705–2717 (2002).
[191]C.-M. Ma *et al.*, "Monte Carlo verification of IMRT dose distributions from a commercial treatment planning optimization system," Phys. Med. Biol. **45**, 2483–2495 (2000).
[192]T. Pawlicki and C. M. Ma, "Monte Carlo simulation for MLC-based intensity-modulated radiotherapy," Med. Dosim. **26**, 157–168 (2001).
[193]P. Francescon, S. Cora, and P. Chiovati, "Dose verification of an IMRT treatment planning system with the BEAM EGS4-based Monte Carlo code," Med. Phys. **30**, 144–157 (2003).
[194]M. Rincon *et al.*, "Monte Carlo conformal treatment planning as an independent assessment," in *Advanced Monte Carlo for Radiation Physics: Proceedings of the Monte Carlo 2000 Meeting, Lisbon*, edited by A. Kling *et al.* (Springer-Verlag, Berlin, 2001), pp. 565–570.
[195]R. Jeraj, P. J. Keall, and J. V. Siebers, "The effect of dose calculation accuracy on inverse treatment planning," Phys. Med. Biol. **47**, 391–407 (2002).
[196]N. Reynaert *et al.*, "The importance of accurate linear accelerator head modelling for IMRT Monte Carlo calculations," Phys. Med. Biol. **50**, 831–846 (2005).
[197]W. Laub, M. Alber, M. Birkner, and F. Nusslin, "Monte Carlo dose computation for IMRT optimization," Phys. Med. Biol. **45**, 1741–1754 (2000).
[198]N. Dogan, J. V. Siebers, P. J. Keall, F. Lerma, Y. Wu, M. Fatyga, J. F. Williamson, and R. K. Schmidt-Ullrich, "Improving IMRT dose accuracy via deliverable Monte Carlo optimization for the treatment of head and neck cancers," Med. Phys. **33**, 4033–4055 (2006).
[199]J. V. Siebers, M. Lauterbach, S. Tong, Q. Wu, and R. Mohan, "Reducing dose calculation time for accurate iterative IMRT planning," Med. Phys. **29**, 231–237 (2002).
[200]A. M. Bergman, K. Bush, M. P. Milette, I. A. Popescu, K. Otto, and C. Duzenli, "Direct aperture optimization for IMRT using Monte Carlo generated beamlets," Med. Phys. **33**, 3666–3679 (2006).
[201]B. De Smedt, B. Vanderstraeten, N. Reynaert, W. De Neve, and H. Thierens, "Investigation of geometrical and scoring grid resolution for Monte Carlo dose calculations for IMRT," Phys. Med. Biol. **50**, 4005–4019 (2005).
[202]J. F. Dempsey, H. E. Romeijn, J. G. Li, D. A. Low, and J. R. Palta, "A Fourier analysis of the dose grid resolution required for accurate IMRT fluence map optimization," Med. Phys. **32**, 380–388 (2005).
[203]J. H. Hubbell, "Review of photon interaction cross section data in the medical and biological context," Phys. Med. Biol. **44**, R1–R22 (1999).
[204]D. V. Rao, S. M. Seltzer, and P. M. Bergstrom, Jr., "Compton scattering cross-sections for individual subshells for a few elements of biological interest in the energy region 5 keV–10 MeV," Radiat. Phys. Chem. **70**, 479–489 (2004).
[205]S. M. Seltzer, in *Monte Carlo Transport of Electrons and Photons*, edited by W. R. Nelson, T. M. Jenkins, A. Rindi, A. E. Nahum, and D. W. O. Rogers (Plenum, New York, 1988), pp. 81–114.
[206]B. A. Fraass, J. Smathers, and J. Deye, "Summary and recommendations of a National Cancer Institute workshop on issues limiting the clinical use of Monte Carlo dose calculation algorithms for megavoltage external beam radiation therapy," Med. Phys. **30**, 3206–3216 (2003).
[207]E. R. Epp, A. L. Boyer, and K. P. Doppke, "Underdosing of lesions resulting from lack of electronic equilibrium in upper respiratory air cavities irradiated by 10 MV x-ray beams," Int. J. Radiat. Oncol. Biol. Phys. **2**, 613–619 (1977).
[208]M. A. Hunt, G. E. Desobry, B. Fowble, and L. R. Coia, "Effect of low-density lateral interfaces on soft-tissue doses," Int. J. Radiat. Oncol. Biol. Phys. **37**, 475–482 (1997).
[209]E. E. Klein, L. M. Chin, R. K. Rice, and B. J. Mijnheer, "The influence of air cavities on interface doses for photon beams," Int. J. Radiat. Oncol. Biol. Phys. **27**, 419–427 (1993).
[210]T. R. Mackie, J. W. Scrimger, and J. J. Battista, "A convolution method of calculating dose for 15-MV x rays," Med. Phys. **12**, 188–196 (1985).
[211]R. Mohan, C. Chui, and L. Lidofsky, "Differential pencil beam dose computation model for photons," Med. Phys. **13**, 64–73 (1986).
[212]C. X. Yu, J. W. Wong, and J. A. Purdy, "Photon dose perturbations due to small inhomogeneities," Med. Phys. **14**, 78–83 (1987).
[213]M. R. Arnfield, C. H. Siantar, J. Siebers, P. Garmon, L. Cox, and R. Mohan, "The impact of electron transport on the accuracy of computed dose," Med. Phys. **27**, 1266–1274 (2000).
[214]F. C. du Plessis, C. A. Willemse, M. G. Lotter, and L. Goedhals, "Comparison of the Batho, ETAR and Monte Carlo dose calculation methods in CT based patient models," Med. Phys. **28**, 582–589 (2001).
[215]A. O. Jones and I. J. Das, "Comparison of inhomogeneity correction algorithms in small photon fields," Med. Phys. **32**, 766–776 (2005).
[216]T. Knoos, E. Wieslander, L. Cozzi, C. Brink, A. Fogliata, D. Albers, H. Nystrom, and S. Lassen, "Comparison of dose calculation algorithms for treatment planning in external photon beam therapy for clinical situations," Phys. Med. Biol. **51**, 5785–5807 (2006).
[217]M. Miften, M. Wiesmeyer, A. Kapur, and C. M. Ma, "Comparison of RTP dose distributions in heterogeneous phantoms with the BEAM Monte Carlo simulation system," J. Appl. Clin. Med. Phys. **2**, 21–31 (2001).
[218]R. Mohan, "Why Monte Carlo?," in *Proceedings of the 12th ICCR*, edited by D. Leavitt (Medical Physics, Salt Lake City, UT, 1997), pp. 16–18.
[219]S. N. Rustgi, A. K. Rustgi, S. B. Jiang, and K. M. Ayyangar, "Dose perturbation caused by high-density inhomogeneities in small beams in stereotactic radiosurgery," Phys. Med. Biol. **43**, 3509–3518 (1998).
[220]P. Carrasco *et al.*, "Comparison of dose calculation algorithms in phantoms with lung equivalent heterogeneities under conditions of lateral electronic disequilibrium," Med. Phys. **31**, 2899–2911 (2004).
[221]J. Coleman, C. Joy, J. E. Park, P. Villarreal-Barajas, P. L. Petti, and B. Faddegon, "A comparison of Monte Carlo and Fermi–Eyges–Hogstrom estimates of heart and lung dose from breast electron boost treatment," Int. J. Radiat. Oncol. Biol. Phys. **61**, 621–628 (2005).
[222]T. Krieger and O. A. Sauer, "Monte Carlo-versus pencil-beam-/collapsed-cone dose calculation in a heterogeneous multi-layer phantom," Phys. Med. Biol. **50**, 859–868 (2005).
[223]W. U. Laub, A. Bakai, and F. Nusslin, "Intensity modulated irradiation of a thorax phantom: Comparisons between measurements, Monte Carlo calculations and pencil beam calculations," Phys. Med. Biol. **46**, 1695–1706 (2001).
[224]E. Spezi, D. G. Lewis, and C. W. Smith, "Monte Carlo simulation and dosimetric verification of radiotherapy beam modifiers," Phys. Med. Biol. **46**, 3007–3029 (2001).
[225]L. Wang, M. Lovelock, and C. S. Chui, "Experimental verification of a CT-based Monte Carlo dose-calculation method in heterogeneous phantoms," Med. Phys. **26**, 2626–2634 (1999).
[226]K. De Vlamynck, H. Palmans, F. Verhaegen, C. De Wagter, W. De Neve, and H. Thierens, "Dose measurements compared with Monte Carlo simulations of narrow 6 MV multileaf collimator shaped photon beams," Med. Phys. **26**, 1874–1882 (1999).
[227]G. A. Ezzell *et al.*, "Guidance document on delivery, treatment planning, and clinical implementation of IMRT: Report of the IMRT Subcommittee of the AAPM Radiation Therapy Committee," Med. Phys. **30**, 2089–2115 (2003).
[228]C. G. Orton, P. M. Mondalek, J. T. Spicka, D. S. Herron, and L. I. Andres, "Benchmark measurements for lung dose corrections for x-ray beams," Int. J. Radiat. Oncol. Biol. Phys. **10**, 2191–2199 (1984).
[229]R. K. Rice, B. J. Mijnheer, and L. M. Chin, "Benchmark measurements for lung dose corrections for x-ray-beams," Int. J. Radiat. Oncol. Biol. Phys. **15**, 399–409 (1988).
[230]P. M. Charland, I. J. Chetty, S. Yokoyama, and B. A. Fraass, "Dosimetric comparison of extended dose range film with ionization measurements in water and lung equivalent heterogeneous media exposed to megavoltage photons," J. Appl. Clin. Med. Phys. **4**, 25–39 (2003).
[231]P. Dunscombe, P. McGhee, and E. Lederer, "Anthropomorphic phantom measurements for the validation of a treatment planning system," Phys. Med. Biol. **41**, 399–411 (1996).
[232]S. Yokoyama, P. L. Roberson, D. L. Litzenberg, J. M. Moran, and B. A. Fraass, "Surface buildup dose dependence on photon field delivery technique for IMRT," J. Appl. Clin. Med. Phys. **5**, 71–81 (2004).
[233]T. Kron, A. Elliot, T. Wong, G. Showell, B. Clubb, and P. Metcalfe, "X-ray surface dose measurements using TLD extrapolation," Med. Phys. **20**, 703–711 (1993).
[234]B. E. Bjarngard, P. Vadash, and T. Zhu, "Doses near the surface in high-energy x-ray beams," Med. Phys. **22**, 465–468 (1995).
[235]A. S. Shiu *et al.*, "Verification data for electron beam dose algorithms," Med. Phys. **19**, 623–636 (1992).
[236]R. A. Boyd, K. R. Hogstrom, J. A. Antolak, and A. S. Shiu, "A measured data set for evaluating electron-beam dose algorithms," Med. Phys. **28**, 950–958 (2001).
[237]K. De Jaeger, M. S. Hoogeman, M. Engelsman, Y. Seppenwoolde, E. M.

F. Damen, B. J. Mijnheer, L. J. Boersma, and J. V. Lebesque, "Incorporating an improved dose-calculation algorithm in conformal radiotherapy of lung cancer: Re-evaluation of dose in normal lung tissue," Radiother. Oncol. **69**, 1–10 (2003).
[238]I. J. Chetty, M. Rosu, F.-M. Kong, C. Lopez, D. S. Tatro, D. L. McShan, B. A. Fraass, and R. K. Ten Haken, "On the correlation of dose-volume-response using Monte Carlo dose calculation in conformal radiation therapy of lung cancer," in *Proceedings of the 14th ICCR*, edited by B.Y. Yi, S. D. Ahn, E. K. Choi, and S. W. Ha (Jeong, Seoul, Korea, 2004), pp. 457–460.
[239]P. E. Lindsay, I. El Naqa, A. Hope, M. Vicic, J. Cui, J. Bradley, and J. O. Deasy, "Retrospective Monte Carlo dose calculations with limited beam weight information," Med. Phys. **34**, 334–346 (2007).
[240]P. J. Keall, J. Siebers, and R. Mohan, "The impact of Monte Carlo dose calculations on treatment outcomes," in *Proceedings of the 13th ICCR*, edited by T. Bortfeld and W. Schlegel (Springer-Verlag, Heidelberg, 2000), pp. 425–427.
[241]N. Reynaert *et al.*, "Monte Carlo treatment planning for photon and electron beams," Radiat. Phys. Chem. **76**, 643–686 (2007).
[242]A. Fogliata, E. Vanetti, D. Albers, C. Brink, A. Clivio, T. Knoos, G. Nicolini, and L. Cozzi, "On the dosimetric behaviour of photon dose calculation algorithms in the presence of simple geometric heterogeneities: Comparison with Monte Carlo calculations," Phys. Med. Biol. **52**, 1363–1385 (2007).
[243]T. Knoos, A. Ahnesjo, P. Nilsson, and L. Weber, "Limitations of a pencil beam approach to photon dose calculations in lung tissue," Phys. Med. Biol. **40**, 1411–1420 (1995).
[244]P. N. McDermott, T. He, and A. DeYoung, "Dose calculation accuracy of lung planning with a commercial IMRT treatment planning system," J. Appl. Clin. Med. Phys. **4**, 341–351 (2003).
[245]M. F. Tsiakalos, K. Theodorou, C. Kappas, S. Zefkili, and J. C. Rosenwold, "Analysis of the penumbra enlargement in lung versus the quality index of photon beams: A methodology to check the dose calculation algorithm," Med. Phys. **31**, 943–949 (2004).
[246]E. D. Yorke, L. Wang, K. E. Rosenzweig, D. Mah, J. B. Paoli, and C. S. Chui, "Evaluation of deep inspiration breath-hold lung treatment plans with Monte Carlo dose calculation," Int. J. Radiat. Oncol. Biol. Phys. **53**, 1058–1070 (2002).
[247]R. Timmerman, L. Papiez, R. McGarry, L. Likes, C. DesRosiers, S. Frost, and M. Williams, "Extracranial stereotactic radioablation: results of a phase I study in medically inoperable stage I non-small cell lung cancer," Chest **124**, 1946–1955 (2003).
[248]L. Wang, E. Yorke, and C. S. Chui, "Monte Carlo evaluation of tissue inhomogeneity effects in the treatment of the head and neck," Int. J. Radiat. Oncol. Biol. Phys. **50**, 1339–1349 (2001).
[249]C. Boudreau, E. Heath, J. Seuntjens, O. Ballivy, and W. Parker, "IMRT head and neck treatment planning with a commercially available Monte Carlo based planning system," Phys. Med. Biol. **50**, 879–890 (2005).
[250]J. Seco, E. Adams, M. Bidmead, M. Partridge, and F. Verhaegen, "Head-and-neck IMRT treatments assessed with a Monte Carlo dose calculation engine," Phys. Med. Biol. **50**, 817–830 (2005).
[251]C. Martens, N. Reynaert, C. De Wagter, P. Nilsson, M. Coghe, H. Palmans, H. Thierens, and W. De Neve, "Underdosage of the upper-airway mucosa for small fields as used in intensity-modulated radiation therapy: A comparison between radiochromic film measurements, Monte Carlo simulations, and collapsed cone convolution calculations," Med. Phys. **29**, 1528–1535 (2002).
[252]F. Verhaegen, I. J. Das, and H. Palmans, "Monte Carlo dosimetry study of a 6 MV stereotactic radiosurgery unit," Phys. Med. Biol. **43**, 2755–2768 (1998).
[253]F. Sánchez-Doblado *et al.*, "Ionization chamber dosimetry of small photon fields: A Monte Carlo study on stopping-power ratios for radiosurgery and IMRT beams," Phys. Med. Biol. **48**, 2081–2099 (2003).
[254]A. Chaves, M. C. Lopes, C. C. Alves, C. Oliveira, L. Peralta, P. Rodrigues, and A. Trindade, "A Monte Carlo multiple source model applied to radiosurgery narrow photon beams," Med. Phys. **31**, 2192–2204 (2004).
[255]J. S. Li *et al.*, "Clinical implementation of intensity-modulated tangential beam irradiation for breast cancer," Med. Phys. **31**, 1023–1031 (2004).
[256]J. J. DeMarco, I. J. Chetty, and T. D. Solberg, "A Monte Carlo tutorial and the application for radiotherapy treatment planning," Med. Dosim. **27**, 43–50 (2002).
[257]A. Leal, F. Sanchez-Doblado, R. Arrans, J. Rosello, E. C. Pavon, and J. I. Lagares, "Routine IMRT verification by means of an automated Monte Carlo simulation system," Int. J. Radiat. Oncol. Biol. Phys. **56**, 58–68 (2003).
[258]G. X. Ding, D. M. Duggan, C. W. Coffey, P. Shokrani, and J. E. Cygler, "First macro Monte Carlo based commercial dose calculation module for electron beam treatment planning—New issues for clinical consideration," Phys. Med. Biol. **51**, 2781–2799 (2006).
[259]D. W. O. Rogers, A. F. Bielajew, and A. E. Nahum, "Monte Carlo calculations of electron beams in standard dose planning geometries," in *Proceedings of the 8th ICCR* (IEEE, New York, 1984), pp. 140–144.
[260]C. Scherf, J. Scherer, and L. Bogner, "Verification and application of the Voxel-based Monte Carlo (VMC++) electron dose module of oncentratrade mark MasterPlan," Strahlenther. Onkol. **183**, 81–88 (2007).
[261]K. R. Shortt, C. K. Ross, A. F. Bielajew, and D. W. O. Rogers, "Electron beam dose distributions near standard inhomogeneities," Phys. Med. Biol. **31**, 235–249 (1986).
[262]E. Wieslander and T. Knoos, "A virtual-accelerator-based verification of a Monte Carlo dose calculation algorithm for electron beam treatment planning in clinical situations," Radiother. Oncol. **82**, 208–217 (2007).
[263]J. Cygler, J. J. Battista, J. W. Scrimger, E. Mah, and J. Antolak, "Electron dose distributions in experimental phantoms: a comparison with 2D pencil beam calculations," Phys. Med. Biol. **32**, 1073–1086 (1987).
[264]J. A. Hayman *et al.*, "Dose escalation in non-small-cell lung cancer using three-dimensional conformal radiation therapy: Update of a phase I trial," J. Clin. Oncol. **19**, 127–136 (2001).
[265]I. J. Chetty, M. Rosu, D. L. McShan, B. A. Fraass, and R. K. Ten Haken, "The influence of beam model differences in the comparison of dose calculation algorithms for lung cancer treatment planning," Phys. Med. Biol. **50**, 801–815 (2005).
[266]F. M. Kong, R. K. Ten Haken, M. J. Schipper, M. A. Sullivan, M. Chen, C. Lopez, G. P. Kalemkerian, and J. A. Hayman, "High-dose radiation improved local tumor control and overall survival in patients with inoperable/unresectable non-small-cell lung cancer: Long-term results of a radiation dose escalation study," Int. J. Radiat. Oncol. Biol. Phys. **63**, 324–333 (2005).
[267]I. J. Chetty, "Monte Carlo treatment planning: The influence of 'variance reduction' techniques (ECUT, PCUT, ESTEP) on the accuracy and speed of dose calculations," Med. Phys. **32**, 2018 (abstract) (2005).
[268]www.irs.inms.nrc.ca/inms/irs/papers/iccr00/iccr00.html.
[269]E. Heath, McGill University (personal communication).
[270]E. Poon and F. Verhaegen, McGill University (personal communication).